Theoret. Comput. Fluid Dynamics (1996) 8: 1–35

Theoretical and Computational Fluid Dynamics

Spectral Transport Model for Turbulence

D.C. Besnard

Centre d'Etudes de Limeil-Valenton,
94195 Villeneuve-St. Georges, Cedex, France

F.H. Harlow, R.M. Rauenzahn, and C. Zemach

Theoretical Division, Los Alamos National Laboratory,
Los Alamos, NM 87544, U.S.A.

Communicated by M.Y. Hussaini

Received 27 May 1992 and accepted 9 December 1994

Abstract. The spectrum of inhomogeneous turbulence is modeled by an approach that is not limited to regimes of large Reynolds numbers or small mean-flow strain rates. In its simplest form and applied to incompressible flow, the model depends on five phenomenological constants defining the strength of turbulence coupling to mean flow, turbulence transport in physical and wave-number space, and mixing of stress-tensor components. The implications for homogeneous isotropic turbulence are investigated in detail and found to correspond well to the conclusions from more fundamental theories. Under appropriate limiting conditions, a turbulent system described by the model will relax over time into a state of approximate spectral equilibrium permitting a reduction to a "one-point" model for the system that is substantially like the familiar K–ε model. This yields preliminary estimates of the present model's parameters and points to the way to improved modeling of flows beyond the applicability of the K–ε method.

1. Introduction

The theoretical modeling of complex turbulent flows, after decades of effort, is still far from adequate. Only the relatively simple one-point transport models (Launder and Spalding, 1972) come close to being useful for simulating flows of practical interest to the engineering community. Among these, models of the "K–ε" family (Launder and Spalding, 1974; Launder *et al.*, 1972) are simple and robust, and have enjoyed the favor of many researchers; however, there are limitations in what such models can describe. K–ε models can deal with flows close to spectral equilibrium, in a sense we define more precisely in this paper. One of their difficulties lies in the dissipation-rate evolution equation. Until the work by Dannevik *et al.* (1987) and Yoshizawa (1987) their derivation could be said to rely mainly on dimensionality arguments. The unknown physics is represented by adjusting the so-called "universal" coefficients appearing in the model.

More general descriptions, including second-order models (Daly and Harlow, 1970), and models allowing for large density variations (Besnard and Harlow, 1988), have also been developed to enlarge the number of flows that can be simulated; however, they suffer from many of the same flaws of the K–ε models, especially that of a spectral equilibrium assumption. In addition, they have a somewhat inflated number of coefficients to be determined by comparison with experiments, again associated with difficulty in obtaining a dissipation-rate evolution equation.

We are interested in flows that are strongly out of equilibrium, for which the models mentioned above are not well suited. One general aim is to obtain a model that does not require a dissipation-rate equation. For nonequilibrium flows, a spectral approach is therefore attractive. Much work of this type has already been done in the case of homogeneous turbulence (Rose and Sulem, 1978). We avoid the extreme complexities of analytical approaches to turbulence, basing this work on a spectral model that includes numerically tractable approximations, and is realistic for inhomogeneous flows.

In our model, as in earlier models applied to homogeneous isotropic turbulence, an initial state of turbulence may develop during a transient period into a self-similar regime in which wave-number distributions acquire a constant, or approximately constant, shape with scales depending on a space-time scaling law. This is the regime referred to above as spectral equilibrium. It presumes (1) turbulent Reynolds numbers large enough to allow a well-defined inertial range in the wave- number spectrum and (2) a cycle time for the dominant eddies that is small compared with mean-flow distortion time, as measured by the time variation of the strain rate. When it persists over time, it makes feasible the approximate description of turbulence by one-point transport models.

This paper focuses on the development of self-similarity and how it leads to a K–ε model. This establishes the relevance and, in some points, the limitations of our model for equilibrium states, and provides a basis for future studies of fluids in rapidly varying transient states. Analysis begins in Section 2 with velocity correlations between points $\mathbf{x}_1$ and $\mathbf{x}_2$. We obtain a spectral model for inhomogeneous turbulence through a Fourier transform acting on the relative coordinate $\mathbf{r} = \mathbf{x}_1 - \mathbf{x}_2$. This technique has been applied by Bertoglio and Jeandel (1987) and Schiestel (1987). Exact operator equations describing the turbulent flow are set forth. They do not form a closed set, and heuristic arguments are given on how to close them, so as to retain most of the features commonly believed to be characteristic of turbulent flows.

A full understanding of the model in the homogeneous limit, including its limitations, would seem essential if more ambitious simulations are to be pursued. Thus, the homogeneous isotropic case was examined in some detail (Besnard *et al.*, 1990). The results are in good agreement with expectations regarding self-similarity, the Kolmogorov dimensional estimates, and so forth. We also describe the transient states and the rate of convergence to self-similarity. A remarkable result is the existence of simple analytical expressions both for the entire self-similar spectrum shape and for the rate of convergence to self-similarity from initial conditions in certain cases. A summary of this analysis is presented in Section 3. In Section 4 a few comments are made about the case of free shear layers (Kelvin–Helmholtz instability) and the convergence of the solution toward self-similarity. Self-similar spectra exist that are close to the spectra obtained in the homogeneous isotropic case.

We can then assess, within the framework of our model, the limits of validity of the K–ε model obtained by considering moments of the model equations, in a postulated self-similar regime. This is done in Section 5. This provides a point of departure for improvements in more demanding circumstances. Finally, Section 6 summarizes our main themes and indicates some directions for extensions of the model.

This paper assumes constant fluid density. Extension to compressible fluids with large density variation in space and time is under investigation.

2. Spectral Model for Inhomogeneous Turbulence

A. Evolution Equation

We study an ensemble of flows of a fluid of constant density ρ and kinematic viscosity ν. The velocity and pressure fields are separated into mean and fluctuating parts:

$$\mathbf{U}(\mathbf{x}, t) = \mathbf{u}(\mathbf{x}, t) + \mathbf{u}'(\mathbf{x}, t), \qquad P(\mathbf{x}, t) = p(\mathbf{x}, t) + p'(\mathbf{x}, t),$$

where $\mathbf{u} = \langle U \rangle$, $p = \langle P \rangle$, and the brackets denote ensemble average. The two-point velocity correlation (generalized Reynolds tensor) is

$$R_{ij}(\mathbf{x}_1, \mathbf{x}_2, t) = \langle u_i'(\mathbf{x}_1, t) u_j'(\mathbf{x}_2, t) \rangle. \tag{2.1}$$

Hereafter, in Section 2, we omit the argument t for brevity. From the Navier–Stokes equation, we can derive (Schiestel, 1987)

$$\frac{\partial R_{ij}(\mathbf{x}_1,\mathbf{x}_2)}{\partial t} = A_{ij}(\mathbf{x}_1,\mathbf{x}_2) - \left\{ B_{ij}(\mathbf{x}_1,\mathbf{x}_2) + C_{ij}(\mathbf{x}_1,\mathbf{x}_2) + \frac{\partial}{\partial x_{1i}}\Pi_j(\mathbf{x}_1,\mathbf{x}_2) + \frac{\partial}{\partial x_{1n}} T_{inj}(\mathbf{x}_1,\mathbf{x}_2) \right\}^{\mathrm{S}}, \tag{2.2}$$

where S means that the enclosed expression is to be symmetrized by adding terms with $i \leftrightarrow j$, $\mathbf{x}_1 \leftrightarrow \mathbf{x}_2$, and

$$A_{ij}(\mathbf{x}_1,\mathbf{x}_2) = \nu(\nabla_1^2 + \nabla_2^2) R_{ij}(\mathbf{x}_1,\mathbf{x}_2), \tag{2.2a}$$

$$B_{ij}(\mathbf{x}_1,\mathbf{x}_2) = \frac{\partial}{\partial x_{1n}} u_n(\mathbf{x}_1) R_{ij}(\mathbf{x}_1,\mathbf{x}_2), \tag{2.2b}$$

$$C_{ij}(\mathbf{x}_1,\mathbf{x}_2) = \frac{\partial}{\partial x_{1n}} u_i(\mathbf{x}_1) R_{nj}(\mathbf{x}_1,\mathbf{x}_2), \tag{2.2c}$$

$$\Pi_j(\mathbf{x}_1,\mathbf{x}_2) = \frac{\langle p'(\mathbf{x}_1) u_j'(\mathbf{x}_2)\rangle}{\rho}, \tag{2.2d}$$

$$T_{inj}(\mathbf{x}_1,\mathbf{x}_2) = \langle u_i'(\mathbf{x}_1) u_n'(\mathbf{x}_1) u_j'(\mathbf{x}_2)\rangle. \tag{2.2e}$$

The incompressibility conditions lead to

$$\frac{\partial u_i}{\partial x_i} = \frac{\partial u_i'}{\partial x_i} = 0, \tag{2.3}$$

$$\frac{\partial}{\partial x_{1i}} R_{ij}(\mathbf{x}_1,\mathbf{x}_2) = \frac{\partial}{\partial x_{2j}} R_{ij}(\mathbf{x}_1,\mathbf{x}_2) = 0, \tag{2.4}$$

$$\frac{\partial}{\partial x_{2j}} \Pi_j(\mathbf{x}_1,\mathbf{x}_2) = \frac{\partial}{\partial x_{2j}} T_{inj}(\mathbf{x}_1,\mathbf{x}_2) = 0. \tag{2.5}$$

The mean-flow equation is

$$\frac{\partial}{\partial t} u_i(\mathbf{x}) = -u_n(\mathbf{x}) \frac{\partial}{\partial x_n} u_i(\mathbf{x}) - \frac{(\partial/\partial x_i) p(\mathbf{x})}{\rho} + \nu \nabla^2 u_i(\mathbf{x}) - \frac{\partial}{\partial x_n} R_{in}(\mathbf{x},\mathbf{x}). \tag{2.6}$$

The expression of the pressure-velocity correlation Π_j in terms of R_{ij} is obtained by solving for p' by computing $\nabla \cdot \partial \mathbf{u}'/\partial t$ and using Green's theorem:

$$\Pi_j(\mathbf{x}_1,\mathbf{x}_2) = \int G(\mathbf{x}_1,\mathbf{x}')\, d\mathbf{x}' \frac{\partial}{\partial x_n'} \frac{\partial}{\partial x_m'} \{2u_n(\mathbf{x}') R_{mj}(\mathbf{x}',\mathbf{x}_2) + T_{mnj}(\mathbf{x}',\mathbf{x}_2)\} \tag{2.7}$$

in which Green's function satisfies

$$-\nabla_1^2 G(\mathbf{x}_1,\mathbf{x}') = \delta(\mathbf{x}_1 - \mathbf{x}')$$

with boundary conditions appropriate to the fluid domain. If the fluid extends through all (three-dimensional) space, we can expect $\Pi_j(\mathbf{x}_1,\mathbf{x}_2)$ to go to zero as $|\mathbf{x}_1|$ increases, $|\mathbf{x}_2|$ being held fixed, and take

$$G(\mathbf{x}_1,\mathbf{x}') = \frac{1}{4\pi|\mathbf{x}_1 - \mathbf{x}'|}. \tag{2.8}$$

An image term could be added for wall effects; we avoid this step for now.

To obtain a spectral model, we first define center and relative coordinates for two-points functions by $\mathbf{x} = \frac{1}{2}(\mathbf{x}_1 + \mathbf{x}_2)$, $\mathbf{r} = \mathbf{x}_1 - \mathbf{x}_2$ and introduce Fourier transforms, as described in detail in Appendix A. The Fourier transform of $R_{ij}(\mathbf{x}_1,\mathbf{x}_2)$ is expressed as

$$R_{ij}(\mathbf{x},\mathbf{k}) = \int e^{-i\mathbf{k}\cdot\mathbf{r}} R_{ij}\left(\mathbf{x} + \frac{\mathbf{r}}{2}, \mathbf{x} - \frac{\mathbf{r}}{2}\right) d\mathbf{r}. \tag{2.9}$$

Let E_{ij} be proportional to the shell-average of R_{ij} over directions of $\mathbf{k}$ for fixed $|\mathbf{k}| = k$, and normalized so that $\int E_{ll}(\mathbf{x}, k)\,dk$ is the turbulent kinetic energy density (i.e., the energy per unit mass) at $\mathbf{x}$. This means

$$E_{ij}(\mathbf{x}, k) = \tfrac{1}{2}\int R_{ij}(\mathbf{x}, \mathbf{k})\frac{k^2\,d\Omega_k}{(2\pi)^3}, \tag{2.10}$$

and, from (A.2), $E_{ij}(\mathbf{x}, k) = E_{ji}(\mathbf{x}, k)$. The one-point Reynolds stress tensor, which is responsible for turbulence effects in (2.6), is related to E_{ij} by

$$R_{ij}(\mathbf{x}, \mathbf{x}) = 2\int_0^\infty E_{ij}(\mathbf{x}, k)\,dk. \tag{2.11}$$

This result suggests the utility of working with $E_{ij}(\mathbf{x}, k)$ as the basic variable in our spectral transport modeling, and this is indeed the approach we take in Section 2.B.

Fourier transforms allow us to re-express (2.2) in $(\mathbf{x}, \mathbf{k})$-space, formulated in terms of nonlocal operator expressions (see Appendix A). The result is (A.12), which is exact, but not complete and requires some approximation for nonlocal terms and for the third-order correlations in order to be tractable. We proceed in the following heuristic way.

We expect $R_{ij}(\mathbf{x}_1, \mathbf{x}_2)$ to vanish as $|\mathbf{r}|$ becomes large, and write L_T as the two-point correlation length or turbulence length scale, i.e., the length such that $R_{ij}(\mathbf{x}_1, \mathbf{x}_2)$ becomes ignorable for $|\mathbf{r}| > L_T$. We assume, in addition, that correlation lengths for third-order correlations are of the order of or less than L_T. We write L_M for the mean-flow length scale. One possible characterization of L_M is that $\mathbf{u}(\mathbf{x} + \Delta\mathbf{x})$ can be approximated by a few terms of a power series in $\Delta\mathbf{x}$ when $|\Delta\mathbf{x}| < L_M$.

Continuing heuristically, we expect length scales dominating mean flow to be, on the average, larger than those dominating the turbulent flow, which is roughly expressible as $L_T < L_M$. A similar rationale is used in Yoshizawa (1984). Turbulent fluctuations are assumed to vary on much smaller scales than the mean flow, both in time and space. A small parameter expansion then leads to a series of spectral equations for which closures are provided using DIA formalism. The operator expression (see Appendix A) can be expanded in series of powers of derivatives.

As shown in Appendix A, the magnitudes of successive terms can be interpreted as proceeding in powers of (L_T/L_M). The first step from the exact evolution equation for R_{ij} to the model is to truncate the derivative expansion, retaining no more than the lowest relevant orders of x- and k-derivatives. The R_{ij} equation reduces to

$$\underbrace{\frac{\partial}{\partial t}R_{ij}(\mathbf{x},\mathbf{k})}_{(0)} = \underbrace{-2\nu k^2 R_{ij}(\mathbf{x},\mathbf{k})}_{(1a)} + \underbrace{\tfrac{1}{2}\nu\nabla^2 R_{ij}(\mathbf{x},\mathbf{k})}_{(1b)} \underbrace{- u_n(\mathbf{x})\frac{\partial}{\partial x_n}R_{ij}(\mathbf{x},\mathbf{k})}_{(2a)} + \underbrace{\frac{\partial u_n}{\partial x_m}k_n\frac{\partial}{\partial k_m}R_{ij}(\mathbf{x},\mathbf{k})}_{(2b)}$$

$$\underbrace{-\frac{\partial u_i}{\partial x_m}R_{mj}(\mathbf{x},\mathbf{k}) - \frac{\partial u_j}{\partial x_m}R_{im}(\mathbf{x},\mathbf{k})}_{(3)} + \underbrace{2\frac{\partial u_n}{\partial x_m}\frac{k_n}{k^2}[k_i R_{mj}(\mathbf{x},\mathbf{k}) + k_j R_{im}(\mathbf{x},\mathbf{k})]}_{(4a)}$$

$$\underbrace{+ i\frac{k_m k_n}{k^2}[k_i T_{mnj}(\mathbf{x},\mathbf{k}) - k_j T_{mni}(\mathbf{x},-\mathbf{k})] + \frac{1}{2}\frac{k_m k_n}{k^2}\left[\frac{\partial}{\partial x_i}T_{mnj}(\mathbf{x},\mathbf{k}) + \frac{\partial}{\partial x_j}T_{mni}(\mathbf{x},-\mathbf{k})\right]}_{(4b)}$$

$$\underbrace{+ \frac{k_m}{k^2}\left\{\frac{\partial}{\partial x_n}[k_i T_{mnj}(\mathbf{x},\mathbf{k}) + k_j T_{mnj}(\mathbf{x},-\mathbf{k})] - \frac{k_n k_l}{k^2}\frac{\partial}{\partial x_l}[k_i T_{mnj}(\mathbf{x},\mathbf{k}) + k_j T_{mni}(\mathbf{x},-\mathbf{k})]\right\}}_{(4c)}$$

$$\underbrace{- ik_n[T_{inj}(\mathbf{x},\mathbf{k}) - T_{jni}(\mathbf{x},-\mathbf{k})]}_{(5a)} \underbrace{- \frac{1}{2}\frac{\partial}{\partial x_n}[T_{inj}(\mathbf{x},\mathbf{k}) + T_{jni}(\mathbf{x},-\mathbf{k})]}_{(5b)}. \tag{2.12}$$

This equation is similar to one obtained previously by Menoret (1982), and used as a starting point by Bertoglio and Jeandel (1987). Our approach furnishes approximations at all orders, which can be obtained from Appendix A. In addition, the terms whose expressions are given in (2.12) can be related to specific physical processes.

Terms (1a) and (1b), respectively, show viscous dissipation and viscous diffusion. The terms (2a), (2b), and (3) represent advection and coupling to mean-flow gradients. The terms (4a–c) arise from pressure–velocity correlations; they include additional mean-flow coupling and triple correlation effects, arising from (2.7). The terms (5a) and (5b) are the triple correlation terms from (2.2e). The triple correlations are responsible for turbulent diffusion in x-space, which arises from the space-divergence terms, as well as for the cascading transfer of turbulence in k-space and the relaxation toward isotropy of the tensor E_{ij}.

B. An Evolution Equation for E_{ij}

We do not model (2.12) directly. Equation (2.11) shows that we need an equation for E_{ij}, as defined by (2.10), to solve the mean-flow equation. Integrating (2.12) over shells in **k**-space in terms (0), (1a), (1b), (2a), and (3) and supplying additional factors as in (2.10) simply replaces R_{ij} by E_{ij}. For the purposes of this paper, we now integrate over the direction of **k** in the other terms as well, leaving only $k = |\mathbf{k}|$ as the wave-number coordinate, and assume that the results may be modeled in terms of mean-flow gradients and the E_{ij}. The limitations imposed by this assumption are still under investigation; at this stage, it is mainly a matter of expediency.

We propose, for each term to be modeled, the simplest, dimensionally correct, rotationally invariant, linear or nonlinear expression satisfying its intrinsic properties.

Within the pressure–velocity correlation expression (terms (4a–c)), only (4a) involves mean-flow gradients. The **k**-space angular integration transforms (4a) into a mean-flow coupling term (MF) for the evolution equation:

$$MF = \frac{\partial u_n}{\partial x_m}(M_{mj}^{ni} + M_{mi}^{nj}), \tag{2.13}$$

where

$$M_{mj}^{ni} = \tfrac{1}{2}\int \frac{2k_n k_i}{k^2} R_{mj}(\mathbf{x}, \mathbf{k}) \frac{k^2\, d\Omega_k}{(2\pi)^3}.$$

The most general modeled form for M_{mj}^{ni} as a linear function of the E-tensor, and respecting the symmetries

$$M_{mj}^{ni} = M_{mj}^{in} = M_{jm}^{ni},$$

is, with the q_i denoting constants, and $E \equiv E_{ll}$,

$$M_{mj}^{ni} = q_1(\delta_{ij}E_{nm} + \delta_{nj}E_{im} + \delta_{im}E_{nj} + \delta_{nm}E_{ij}) + q_2\delta_{ni}E_{mj} + q_3\delta_{mj}E_{ni} + q_4\delta_{ni}\delta_{mj}E + q_5(\delta_{nm}\delta_{ij} + \delta_{nj}\delta_{mi})E.$$

Then (2.13) can be rewritten as

$$MF = c_B\left(\frac{\partial u_i}{\partial x_m}E_{mj} + \frac{\partial u_j}{\partial x_m}E_{im} - \tfrac{2}{3}\delta_{ij}\frac{\partial u_n}{\partial x_m}E_{nm}\right) + c_{B1}\left(\frac{\partial u_n}{\partial x_i}E_{nj} + \frac{\partial u_n}{\partial x_j}E_{in} - \tfrac{2}{3}\delta_{ij}\frac{\partial u_n}{\partial x_m}E_{nm}\right)$$
$$+ c_{B2}\left(\frac{\partial u_i}{\partial x_j} + \frac{\partial u_j}{\partial x_i}\right)E + c_X\delta_{ij}\frac{\partial u_n}{\partial x_m}E_{nm}, \tag{2.13a}$$

where

$$c_B = q_1 + q_2, \qquad c_{B1} = q_1 + q_3, \qquad c_{B2} = q_4 + q_5, \tag{2.14}$$

and

$$c_X = \frac{2(5q_1 + q_2 + q_3)}{3}.$$

However, MF must be traceless in i, j, and hence $c_X = 0$. This is required to secure energy balance between mean and turbulent energies.

Additional constraints on the q_i are implied by the conditions

$$M_{mj}^{ii} = 2E_{mj}, \qquad M_{mj}^{nj} = 0. \tag{2.15}$$

The second relation follows from $k_j R_{mj} = 0$, which is an approximate version of the incompressibility condition equation (A.5) resulting from neglect of $\partial/\partial x_j$ relative to k_j. The consequence for MF is

$$c_{B1} = 8c_B - 6, \qquad c_{B2} = -3c_B + \tfrac{11}{5}. \tag{2.16}$$

More generally, all the q_i are related to c_B if we comply with (2.15):

$$q_1 = -3c_B + 2, \qquad q_2 = 4c_B - 2, \qquad q_3 = 11c_B - 8, \qquad q_4 = -5c_B + \tfrac{18}{5}, \qquad q_5 = 2c_B - \tfrac{7}{5}.$$

This discussion is substantially the same as that given by Launder *et al.* (1975) (whose c_2 equals our q_3) for the one-point modeling of the pressure–strain correlation. In particular, the relations among the coefficients of the three coupling terms stem from the same physical circumstance, namely, the presumed slower variation of the relevant functions with **x** than with **r**, which we have expressed as $L_T/L_M < 1$.

In term (2b) the order of k_n and $\partial/\partial k_m$ can be reversed. Denote the contribution to $\partial E_{ij}/\partial t$ by MF'. By Gauss' theorem,

$$\begin{aligned} MF' &= \tfrac{1}{2}\int \frac{\partial}{\partial k_m}\left[\frac{\partial u_n}{\partial x_m} k_n R_{ij}(\mathbf{x},\mathbf{k})\right]\frac{k^2\, d\Omega_k}{(2\pi)^3} \\ &= \frac{1}{2}\frac{\partial}{\partial k}\int \frac{\partial u_n}{\partial x_m} k_n \frac{k_m}{k} R_{ij}(\mathbf{x},\mathbf{k})\frac{k^2\, d\Omega_k}{(2\pi)^3} \\ &= \frac{1}{2}\frac{\partial}{\partial k}\left(k\frac{\partial u_n}{\partial x_m} M_{ji}^{nm}\right). \end{aligned}$$

Using the structure of the M-tensor developed above, we get

$$\begin{aligned} \frac{1}{2}\frac{\partial u_n}{\partial x_m} M_{ji}^{nm} &= c_F\left(\frac{\partial u_i}{\partial x_m} E_{mj} + \frac{\partial u_j}{\partial x_m} E_{im} - \tfrac{2}{3}\delta_{ij}\frac{\partial u_n}{\partial x_m} E_{nm}\right) + c_F\left(\frac{\partial u_n}{\partial x_i} E_{nj} + \frac{\partial u_n}{\partial x_j} E_{in} - \tfrac{2}{3}\delta_{ij}\frac{\partial u_n}{\partial x_m} E_{nm}\right) \\ &\quad + c_{F1}\left(\frac{\partial u_i}{\partial x_j} + \frac{\partial u_j}{\partial x_i}\right) E + c_{F2}\delta_{ij}\frac{\partial u_n}{\partial x_m} E_{nm}, \end{aligned}$$

where

$$c_F = \frac{-3c_B}{2} + 1, \qquad c_{F1} = c_B - \tfrac{7}{10}, \qquad c_{F2} = \frac{7c_B}{2} - \frac{8}{3}. \tag{2.17}$$

MF' is conservative because of the k-derivative and need not be traceless with respect to i, j. It provides for transport of energy in k-space induced by mean flow.

Terms (4b) and (5a) involve only turbulent correlations, and do not vanish for homogeneous isotropic turbulence. They are interpreted as describing the flux of E_{ij} in k-space. They involve two different processes, cascading transfer between scales, denoted by KT, and return to isotropy in physical space. This latter term does not transfer energy between scales, but instead rearranges the distribution of stress among the components of E_{ij}, and contributes to the decay of off-diagonal elements. It corresponds to the part in the pressure–velocity correlation, in single-point turbulence transport modeling, that contracts to zero and therefore does not alter the total energy. Here, we model this term, denoted as TM (tensor mixing), by simple linear return toward isotropy:

$$TM = c_M k\sqrt{kE}\left[\tfrac{1}{3}E\delta_{ij} - E_{ij}\right],$$

where $E \equiv E(\mathbf{x}, k) = E_{ll}(\mathbf{x}, k)$ is again the turbulent energy density.

To model the cascading transfer term KT, we can choose from the most sophisticated models, e.g., the distant-interaction algorithm (DSTA) (Kraichnan, 1987) and the Eddy-Damped Quasi-Normal Markovian model (EDQNM) (Lesieur, 1987), down to the simple diffusion approximations for the flux of energy in k-space of Leith (1967, 1968), or use intermediate ones, such as that of Heisenberg (1948). Yoshizawa (1984) used the DIA formalism to close a truncated series of spectral equations and could derive "one-point" transport equations. This other route to one-point transport models, although effective at providing spectrally integrated equations, is very complex. Indeed, the spectral equations that are the basis for Yoshizawa's derivation defy any analysis and, therefore, do not provide the kind of insight in turbulence spectral behavior that we can extract from our model equations. Although the *physical* transfer of energy in k-space is nonlocal, we restrict our model for phenomenological purposes, to a combined wave-like and diffusion-like approximation. We show in Section 3 that this type of phenomonology gives results closely in agreement with those of EDQNM for homogeneous isotropic turbulence. Thus, extending the work of

Leith, we propose

$$KT = -c_1 \frac{\partial}{\partial k}(k^2 \sqrt{kE} E_{ij}) + c_2 \frac{\partial}{\partial k}\left(k^3 \sqrt{kE} \frac{\partial E_{ij}}{\partial k} \right),$$

where c_1 and c_2 are constants.

As one referee suggested, more physically motivated models may be chosen, such as $(\int_0^k p^2 E(p)\, dp)^{1/2}$ instead of $(k^3 E(k))^{1/2}$. We explored this numerically. The results showed little difference from those obtained with our local approximation, and support our initial choice, in regard to cascade of energy and stress. The suggestion can be important for, e.g., cascade of a passive scalar, however.

The last terms to be modeled are (4c) and (5b). They are conservative in physical space, and were modeled as turbulent self-diffusion by Daly and Harlow (1970). A symmetrized spectral analog would be

$$c_D \frac{\partial}{\partial x_n}\left[D_{nl} \frac{\partial}{\partial x_l} E_{ij} + D_{jl} \frac{\partial}{\partial x_l} E_{ni} + D_{il} \frac{\partial}{\partial x_l} E_{jn} \right].$$

The diffusion coefficient D_{nl} would be expressed as

$$D_{nl} = \int_0^\infty \sqrt{\frac{k}{E}} \frac{E_{nl}}{k^2}\, dk.$$

For present purposes we simplify this, using, instead, a turbulent diffusion (TD) term

$$TD = c_D \frac{\partial}{\partial x_n}\left(\nu_T \frac{\partial E_{ij}}{\partial x_n} \right),$$

depending on a turbulent viscosity coefficient ν_T,

$$\nu_T(\mathbf{x}) = \int_0^\infty \frac{\sqrt{kE(\mathbf{x}, k)}}{k^2}\, dk. \tag{2.18}$$

The spectral transport model equation for E_{ij}, with the choices made above, will now be stated in full. The couplings of mean-flow gradient and energy tensor can be expressed with the aid of three traceless tensors, defined as follows:

$$A_{ij} = \frac{\partial u_i}{\partial x_n} E_{nj} + \frac{\partial u_j}{\partial x_n} E_{in} - \tfrac{2}{3}\delta_{ij} \frac{\partial u_n}{\partial x_m} E_{nm}, \tag{2.19a}$$

$$B_{ij} = \frac{\partial u_n}{\partial x_i} E_{nj} + \frac{\partial u_n}{\partial x_j} E_{in} - \tfrac{2}{3}\delta_{ij} \frac{\partial u_n}{\partial x_m} E_{nm}, \tag{2.19b}$$

$$C_{ij} = \left(\frac{\partial u_i}{\partial x_j} + \frac{\partial u_j}{\partial x_i} \right) E. \tag{2.19c}$$

Also, let $\mathbf{V}$ be the operator in (2.12) depending on ν and let $\mathbf{T}$ be the operator that defines transport in $\mathbf{x}$-space and $\mathbf{k}$-space:

$$\mathbf{V} = \nu(-2k^2 + \tfrac{1}{2}\nabla^2), \tag{2.19d}$$

$$\mathbf{T} = c_D \frac{\partial}{\partial x_n} \nu_T \frac{\partial}{\partial x_n} - c_1 \frac{\partial}{\partial k} k^2 \sqrt{kE} + c_2 \frac{\partial}{\partial k} k^3 \sqrt{kE} \frac{\partial}{\partial k}. \tag{2.19e}$$

Then

$$\frac{\partial E_{ij}}{\partial t} + u_n \frac{\partial E_{ij}}{\partial x_n} = \mathbf{V}[E_{ij}] + \mathbf{T}[E_{ij}] - \left(\frac{\partial u_i}{\partial x_n} E_{nj} + \frac{\partial u_j}{\partial x_n} E_{in} \right) + c_B A_{ij} + c_{B1} B_{ij} + c_{B2} C_{ij}$$
$$+ \frac{\partial}{\partial k}\left[c_F A_{ij} + c_F B_{ij} + c_{F1} C_{ij} + c_{F2} \delta_{ij} \frac{\partial u_n}{\partial x_m} E_{nm} \right] + c_M k \sqrt{kE}(\tfrac{1}{3} E \delta_{ij} - E_{ij}). \tag{2.20}$$

There are five indepenent dimensionless phenomenological constants in this model, namely, c_B, c_D, c_1, c_2, and c_M. We expect these constants to be positive and of order unity, or less. (However, we do consider

$c_1 < 0$ in Section 3.) They have to be determined through additional constraints, and/or empirical fits to experiments. Five additional constants, c_{B1}, c_{B2}, c_F, c_{F1}, and c_{F2} are determined from c_B by (2.16) and (2.17).

It is also useful to separate E_{ij} into two parts,

$$E_{ij} = \tfrac{1}{3}E\delta_{ij} + \tilde{E}_{ij}, \tag{2.21}$$

so that $\tilde{E}_{ij}$ is traceless and represents the deviation of the energy tensor from isotropy. (Of course, $\tilde{E}_{ij} = E_{ij}$ for $i \neq j$.) $\tilde{E}_{ij}$ is called the "anisotropic part" of E_{ij}. Then, referring to (2.19), we get

$$A_{ij} = \tilde{A}_{ij} + \tfrac{1}{3}C_{ij},$$

$$B_{ij} = \tilde{B}_{ij} + \tfrac{1}{3}C_{ij},$$

where $\tilde{A}_{ij}$, $\tilde{B}_{ij}$ are formed like A_{ij}, B_{ij}, but with the E tensor replaced by the $\tilde{E}$ tensor.

Evolution equations for E and $\tilde{E}_{ij}$ are obtained by applying

$$E = \operatorname{trace} E_{ij}, \qquad \tilde{E}_{ij} = (\delta_{ia}\delta_{jb} - \tfrac{1}{3}\delta_{ij}\delta_{ab})E_{ab}$$

in turn to (2.20), then substituting (2.21) into the results and recalling $\partial u_n/\partial x_n = 0$. This yields

$$\frac{\partial E}{\partial t} + u_n\frac{\partial E}{\partial x_n} = \mathbf{V}[E] + \mathbf{T}[E] - 2\frac{\partial u_n}{\partial x_m}\tilde{E}_{nm} + 3c_{F2}\frac{\partial}{\partial k}\left(k\frac{\partial u_n}{\partial x_m}\tilde{E}_{nm}\right), \tag{2.22a}$$

$$\frac{\partial \tilde{E}_{ij}}{\partial t} + u_n\frac{\partial \tilde{E}_{ij}}{\partial x_n} = \mathbf{V}|\tilde{E}_{ij}| + \mathbf{T}|\tilde{E}_{ij}| + (c_B - 1)\tilde{A}_{ij} + c_{B1}\tilde{B}_{ij} - \frac{2C_{ij}}{15} + \frac{\partial}{\partial k}k\left[c_F\tilde{A}_{ij} + c_F\tilde{B}_{ij} - \frac{C_{ij}}{30}\right] - c_M k\sqrt{kE}\tilde{E}_{ij}. \tag{2.22b}$$

There are, admittedly, a large number of terms in these evolution equations. However, each of the physical processes which the model addresses, namely, advection, viscous diffusion, viscous dissipation, turbulent diffusion in **x**-space, cascade in k-space, energy exchange between mean and turbulent flow, and exchange of stress among energy tensor components, is an essential part of turbulent processes and must be represented in some manner.

In an earlier version of this model (Besnard *et al.*, 1990), we disregarded the c_{B1} and c_{B2} terms in (2.20) for the sake of simplicity. This would be consistent with Launder *et al.* (1975), who found that in fitting their one-point model to experiment, the c_B-type term is dominant. We also disregarded the c_F, c_{F1}, and c_{F2} terms for the same reason. The simplified model was successfully applied in Gore *et al.* (1991). As noted in Section 5, neglecting these terms does not have a visible effect on K–ε equations deduced under the conditions of spectral equilibrium, but subsequent work (Clark, 1991; Clark and Zemach, 1991) showed that these terms in question are needed to explain wind-tunnel experiments in which the turbulence has not reached spectral equilibrium.

3. Self-Similar Regimes: Homogeneous Isotropic Turbulence

In this section we summarize results for homogeneous isotropic turbulence. Details can be found in Besnard *et al.* (1990).

A. The Parameters c_1 and c_2

We consider evolution of the turbulent energy distribution $E(k, t)$ from an initial space-independent distribution $E(k, 0)$, when the mean-flow gradients vanish. The E equation reduces to a homogeneous partial differential equation (homogeneous isotropic PDE),

$$\frac{\partial E}{\partial t} = -2\nu k^2 E - c_1\frac{\partial}{\partial k}(k^{5/2}E^{3/2}) + c_2\frac{\partial}{\partial k}\left(k^{7/2}E^{1/2}\frac{\partial E}{\partial k}\right), \tag{3.1}$$

uncoupled to the other tensor components.

If (3.1) is not supplemented by an input energy term, it describes homogeneous isotropic decay. The equation of energy balance is

$$\frac{d}{dt}\int_0^\infty E(k,t)\,dk = -2\nu\int_0^\infty k^2 E\,dk - [\mathbf{F}]_{k\to\infty}, \tag{3.2}$$

where $\mathbf{F}(k,t)$, the flux of E, is given by

$$\mathbf{F} = c_1 k^{5/2}E^{3/2} - c_2 k^{7/2}E^{1/2}\frac{\partial E}{\partial k}.$$

If there is an inertial range in the k-spectrum where $E \approx E_\infty(t)k^{-5/3}$, then in that range

$$\mathbf{F} \approx E_\infty^{3/2}\left(c_1 + \frac{5c_2}{3}\right). \tag{3.3}$$

Compare with the Kolmogorov (1941) equation for three-dimensional turbulence, $E = C_K\varepsilon^{2/3}k^{-5/3}$, where the dissipation rate ε is identified with $\mathbf{F}$ and the Kolmogorov constant C_K is known experimentally to be near 1.5. This constrains the physical values of c_1, c_2 for three-dimensional turbulence:

$$c_1 + \frac{5c_2}{3} = C_K^{-3/2} \approx 0.54. \tag{3.4}$$

The advection term of (3.1) describes energy transfer toward higher k if $c_1 > 0$ and towards lower k if $c_1 < 0$. The constant c_2 multiplies a diffusion term and may not be negative. For physically reasonable spectra, c_2 should not be zero, either, as diffusion is needed to provide energy transfer in both k directions. (If $c_2 = 0$, (3.1) becomes the model of Kovasznay (1948). It is solvable by the method of characteristics, and defines characteristic curves $k = k(t)$ that diverge to $k = \infty$ at finite t.)

The shape of the E-spectrum becomes time independent at large t, while its normalization and motion on the k-axis follow power laws in time. This self-similar spectrum depends on the ratio $c = c_1/c_2$ and, broadly speaking, three regimes are found. For $c \geqslant -\frac{5}{3}$, there is a $k^{-5/3}$ inertial range as is appropriate for three-dimensional turbulence. Figure 1 shows an example of such a spectrum. The shape itself is independent of c_1 and c_2, or weakly dependent, for k of the order of, or exceeding, the dominant-eddy wave numbers. Fitting c to experimental data on homogeneous turbulence would then depend on the spectrum shape for smaller k, on viscosity effects, on the rate of convergence to a self-similar state, and on other time-dependent phenomena. For $c < -3$, there is a k^{-3} inertial range (which becomes $k^{-3}\log^2 k$ for $c = -3$). For the intermediate range $-3 < c < -\frac{5}{3}$, the range-k behaviour (for $\nu = 0$) is like k^c.

To consider enstrophy conservation, we re-express (3.1) as

$$\frac{\partial(k^2E)}{\partial t} = -2\nu k^4 E - \frac{\partial}{\partial k}\mathbf{F}_{\text{ens}} + 2(c_1 + 3c_2)k^{7/2}E^{3/2},$$

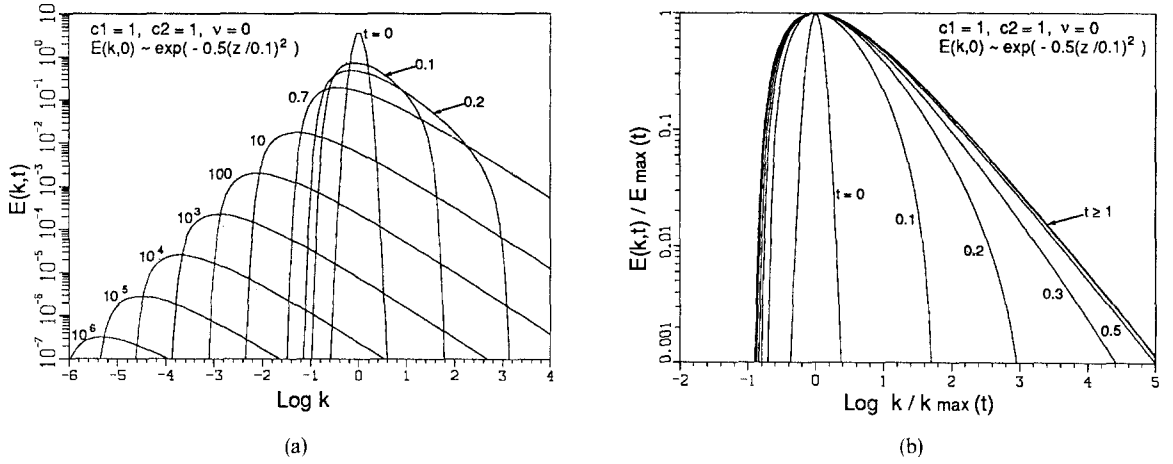

Figure 1. Evolution plot and shape plot of the decay of the homogeneous isotropic turbulent energy distribution evolving from a narrow initial distribution (with $z = \log k$), for $c = c_1/c_2 = 1$.

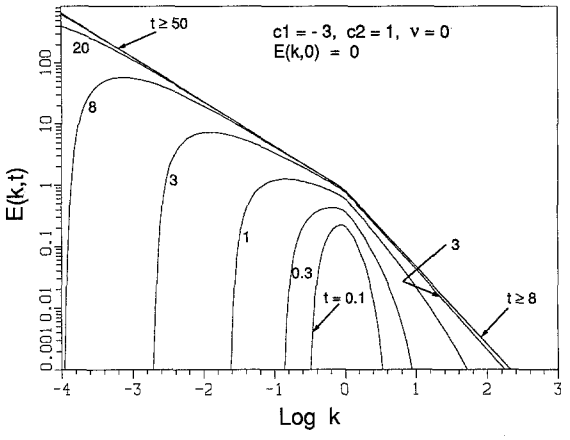

Figure 2. Increase and transport of energy driven by a constant energy source concentrated at $k = 1$ for $c = -3$.

where the flux of enstrophy is given by

$$\mathbf{F}_{\text{ens}} = \left(c_1 + \frac{4c_2}{3}\right) k^{9/2} E^{3/2} - c_2 k^{11/2} E^{1/2} \frac{\partial E}{\partial k}.$$

Thus the homogeneous isotropic PDE conserves enstrophy, apart from viscous dissipation, provided that $c = -3$. This was the choice of Leith (1968) for two-dimensional turbulence. Figure 2 shows evolution of the spectrum from $E(k, 0) = 0$ for such a case.

Previous studies (Leith, 1968; Heisenberg, 1948; Kolmogorov, 1941; Kraichnan, 1967) have suggested a k^{-3} inertial range for two-dimensional turbulence in various modes or perhaps $k^{-3}(\log k)^{-1/3}$, as obtained by Kraichnan (1971). For this reason, and because of enstrophy conservation in appropriate two-dimensional limits of the Navier–Stokes equation, it is tempting to regard the spectral transport model with $c_1/c_2 = -3$ as a candidate model in a two-dimensional limit. However, we are not ready to claim applicability to two-dimensional flows. Other studies and simulations (Basdevant *et al.* 1981; Herring and McWilliams, 1985; Gilbert, 1988; Brachet *et al.*, 1988) indicate behavior varying betweek k^{-3} and k^{-4}, depending on input conditions and the stage of turbulent development. Because the mechanisms for three-dimensional cascade and two-dimensional inverse cascade differ, the applicability of our approach in one context would not necessarily imply applicability in the other.

If a modification of isotropic turbulence dynamics in which a finite energy-containing region of k-space is adiabatically isolated is considered, then the equilibrium energy is equipartitioned, that is, $E(k) \sim k^2$. The same modification of the model dynamics leads to $E(k) \sim k^c$ for the three-dimensional regime, $c \geq -\frac{5}{3}$. This lead Leith, in his 1967 paper, to set (in our notation) $c = 2$. Together with $C_{\mathrm{K}} = 1.5$, this implies $c_1 = 0.297$, $c_2 = 0.148$.

The self-similar spectrum shape depends qualitatively on $E(k, 0)$. If $E(k, 0)$ goes like a power of k near the k-origin, this power behavior may persist in the steady state. Consider a spectrum following a power law at the origin,

$$E(k, 0) \sim k^n e^{-n(k/k^*)^2/2}. \tag{3.5}$$

Figures 3(a) and (b) are evolution plots for $n = 2$ and $n = 4$, respectively. Figures 3(c) and (d) show the corresponding shape-plots. Except for $k \ll k_{\max}$, these curves have much the same character as in Figure 1. There is, however, a persistence of k^n behavior for small k, reflecting the k-dependence enforced by dimensional analysis (the effective diffusion coefficient has a factor of $k^{7/2}$). If $E(k, 0)$ is sharply localized about a positive k-value, $E(k, t)$ may diffuse toward $k = 0$ as a "front," and, for all t, there may be a finite interval about the k-origin in which E vanishes.

In Section 3.D below, we encounter spectra that cut off on the right, essentially vanishing above the dissipation range, when $\nu > 0$. These cut-off behaviors are unsurprising in a nonlinear transport model; see, for example, studies for the porous media equation by Gilding and Peletier (1977) and Gilding (1980). Cut-offs are unlikely to occur in nature because of the *nonlocal* interactions among eddies. Thus, our model

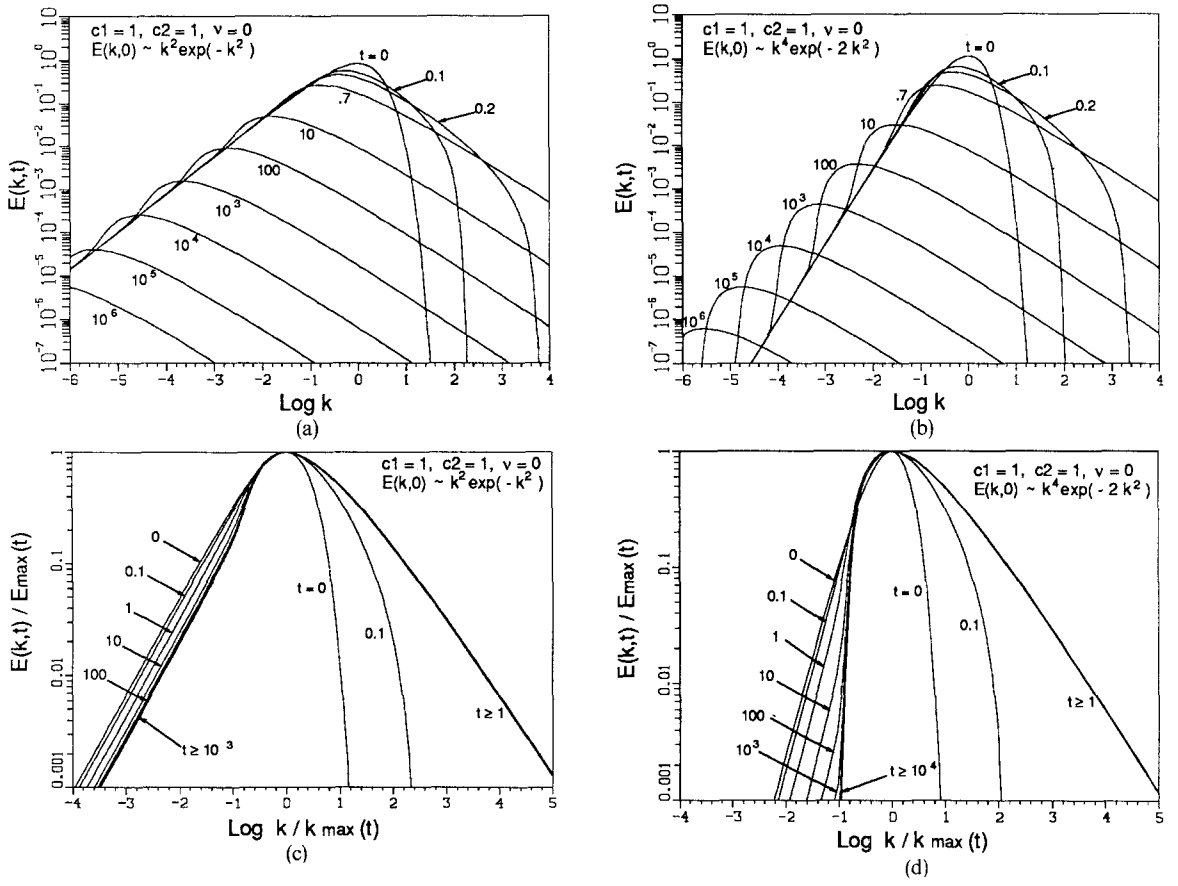

Figure 3. Decays for distributions that initially follow power laws $E \sim k^2$ and $E \sim k^4$, respectively, for small k.

may be comparatively less realistic in the extreme limits $k \to 0$ and $k \to \infty$, though errors in these limits may be unimportant.

B. Self-Similar Form for $E(k, t)$

The time independence of spectrum shape for sufficiently large t suggests that stable solutions to (3.1) exist in the self-similar form

$$E(k, t) = K(t)L(t)f(kL(t)). \tag{3.6}$$

Equation (3.6) is equivalent to the assumption of Kármán and Howarth (1938), expressed in wave-number space.

$L(t)$ appears as a length for k. Set $\xi = kL(t)$, $\xi_{\max} = k_{\max}(t)L(t)$ for the value of ξ that gives f its maximum $f_{\max}$. The scales for the three factors in (3.6) can be set by the normalizations

$$\xi_{\max} = 1, \quad \int_0^\infty f(\xi)\, d\xi = 1. \tag{3.7}$$

Hence, we have

$$L(t) = \frac{1}{k_{\max}(t)}, \qquad \xi = \frac{k}{k_{\max}(t)}, \qquad K(t) = \int_0^\infty E(k, t)\, dk, \tag{3.8}$$

so that $K(t)$ is the total turbulent kinetic energy.

Substituting the self-similar form (3.6) into (3.1), with $\nu = 0$, we get

$$K^{-3/2}L\frac{dK}{dt}f + K^{-1/2}\frac{dL}{dt}\frac{d}{d\xi}(\xi f) = -c_1\frac{d}{d\xi}(\xi^{5/2}f^{3/2}) + c_2\frac{d}{d\xi}\left(\xi^{7/2}f^{1/2}\frac{df}{d\xi}\right). \tag{3.9}$$

There are two ways to reconcile the t- and ξ-dependence of this equation.

First, we may have

$$\frac{d}{d\xi}(\xi f) = \rho f$$

and

$$K^{-3/2} L \frac{dK}{dt} + K^{-1/2} \frac{dL}{dt} \rho = \sigma,$$

where ρ, σ are constants. Then $f(\xi) \sim \xi^{\rho - 1}$. The left- and right-hand sides of (3.9) go, respectively, like $\xi^{\rho - 1}$ and $\xi^{3\rho/2}$. This implies $\rho = -2$ and $f(\xi) \sim \xi^{-3}$ for all ξ. We reject this as a physically unreasonable shape for the (entire) energy spectrum, although the homogeneous isotropic PDE would be satisfied. In particular, neither part of (3.7) can be satisfied.

Second, we may have

$$K^{-3/2} \frac{dK}{dt} L = -\alpha, \tag{3.10a}$$

$$K^{-1/2} \frac{dL}{dt} = \beta. \tag{3.10b}$$

Then we obtain an ordinary differential equation, which we call the homogeneous isotropic ODE:

$$\frac{d}{d\xi}\left[c_2 \xi^{7/2} f^{1/2} \frac{df}{d\xi} - c_1 \xi^{5/2} f^{3/2} - \beta \xi f \right] + \alpha f = 0, \tag{3.11}$$

where α, β are constants. This is the alternative that is realized for large t in the numerical solutions shown above.

Equations (3.10) can be combined to give $d(K^{-1/2} L)/dt = \frac{1}{2}\alpha + \beta$, whence

$$K^{-1/2}(t) L(t) = (\tfrac{1}{2}\alpha + \beta)(t + t_0), \tag{3.12a}$$

and then

$$L(t) = L_0 \left(1 + \frac{t}{t_0} \right)^{\beta/((1/2)\alpha + \beta)}, \tag{3.12b}$$

$$K(t) = K_0 \left(1 + \frac{t}{t_0} \right)^{-\alpha/((1/2)\alpha + \beta)}. \tag{3.12c}$$

The integration constants L_0, K_0, t_0 are related by

$$K_0^{-1/2} L_0 = (\tfrac{1}{2}\alpha + \beta) t_0. \tag{3.12d}$$

Positive β corresponds to $L(t)$ increasing in time, and $k_{\max}(t)$ decreasing in time. Positive α corresponds to $K(t)$ decreasing in time. Integrating (3.11) over ξ yields

$$\alpha = \lim_{\xi \to \infty} \left[c_1 \xi^{5/2} f^{3/2} - c_2 \xi^{7/2} f^{1/2} \frac{df}{d\xi} + \beta \xi f \right]. \tag{3.13}$$

For a spectrum of self-similar form that goes like $k^{-5/3}$ for $k \to \infty$, we must then have

$$f(\xi) \to f_\infty \xi^{-5/3} \qquad \text{as} \quad \xi \to \infty, \qquad f_\infty = \text{constant}, \tag{3.14}$$

and

$$\alpha = f_\infty^{3/2} \left(c_1 + \frac{5 c_2}{3} \right). \tag{3.15}$$

However, if $E(k, t) \to 0$ faster than $k^{-5/3}$ as $k \to \infty$, then $K(t)$ is constant in time, and, either by (3.12b) or (3.13), $\alpha = 0$. This implies $L(t) \sim (t + t_0)$ and $k_{\max}(t) \sim (t + t_0)^{-1}$. Equation (3.11) is a second-order ODE depending on three parameters, which may be taken as the ratios $c = c_1/c_2$, $a = \alpha/\beta$, and β/c_2. We regard c and a as initially specified parameters, and β/c_2 to be determined concurrently with the solution so as to satisfy the first scale convention of (3.7). The time dependences of $K(t)$, $L(t)$, and hence $k_{\max}(t)$ depend only on the a-ratio, not on α or β separately. Note, also, that if $f(\xi)$ is assumed to have a power-law dependence as $\xi \to 0$, then the behavior of (3.11) in this limit shows it must be $f(\xi) \sim \xi^{a-1}$. Then $E(k, t) \sim k^{a-1}$ as $k \to 0$.

The relations between the power-law at $k=0$, if the self-similar state obeys one, and the time dependences of its total energy and length scale are the same as those in the similarity solutions of Kármán and Howarth (1938) and of all later authors and follow from scale invariance. When $E(k, 0)$ goes like k^n near $k=0$, the numerical experiments indicate the following evolution: the region of maximum $E(k, t)$ and the inertial range on the right converge to a self-similar mode on about the same time scale as for an initial narrow Gaussian distribution. If $n+1<\frac{1}{2}(3c+5)$, the distribution as a whole relaxes, on a slower time scale, to a self-similar state with $a=n+1$, which governs the time dependence of $K(t)$ and $L(t)$, and $E\sim k^n$ for $k\to 0$. If $n+1\geq\frac{1}{2}(3c+5)$, the large time value of a is $\frac{1}{2}(3c+5)$, and E converges to the cut-off spectrum. Equation (3.12c) implies

$$-\frac{K(t)}{dK/dt}=\frac{1+\frac{1}{2}a}{a}(t+t_0). \tag{3.16}$$

The solution of (3.16) for the same parameters as Figure 1 has a vertical asymptote at $t^*=0.32$, and t^* is the "catastrophe time" of Brissaud *et al.* (1973). For $t<t^*$, the decay conserves energy and $dK/dt=0$; afterward, energy is lost at $k=\infty$, if it is not dissipated at large k by a residual nonzero viscosity, and the enstrophy integral diverges.

C. Exact Spectra for the Self-Similar Stage

Computations show that many solutions of (3.1) share certain simple characteristics. We could reproduce and extend these results utilizing invariance under scale transformations (for details see Besnard *et al.*, 1990). The underlying ideas are well explained by Bluman and Cole (1974). We now summarize the main results that we obtained.

1. *Case* $c\geq-\frac{5}{3}$. When the homogeneous isotropic PDE is initialized with a narrow spectrum shape, the self-similar state that emerges is characterized by $a=\frac{1}{2}(3c+5)$. We have

$$f(\xi)=\frac{10}{9}\frac{1}{\xi^3}\left(\xi^{2/3}-\frac{5}{9}\right)^2, \qquad \left(\frac{5}{9}\right)^{3/2}\leq\xi. \tag{3.17}$$

This spectrum shape is a universal function independent of c_1 and c_2, provided only that $c+\frac{5}{3}\geq 0$.

The corresponding energy density is determined by two parameters, which can be taken as the cut-off wave number k_0 at $t=0$ and the "waiting time" t_0 of (3.12). Adapting (3.6) and (3.12) to this case, and writing E_s for this solution to the homogeneous isotropic PDE, we have, at $t=0$,

$$\begin{aligned} E_s(k, 0; k_0, t_0)&=\frac{1}{(c_1+3c_2)^2 t_0^2}\frac{1}{k^3}\left[\left(\frac{k}{k_0}\right)^{2/3}-1\right]^2, \qquad k_0\leq k,\\ &=0, \qquad k<k_0. \end{aligned} \tag{3.18}$$

From (3.26), we get $E_s(k, t; k_0, t_0)$ by the replacements

$$k_0\to k_0\left(1+\frac{t}{t_0}\right)^{-1/3(c+3)}, \qquad t_0\to t_0+t. \tag{3.19}$$

Figure 4 shows shape plots computed from (3.11) for a range of a-values at fixed c, and for a range of c-values at fixed a. Except for the variation from power-law to cut-off behavior on the left, the plots are insensitive to the parameters a and c. A fairly accurate explicit formula for the similarity shape for any a and c can be found without computer aid by matching the explicit cut-off solution (3.17) to ξ^{a-1} behavior at small ξ (see Besnard *et al.*, 1990).

2. *Case* $c<-\frac{5}{3}$. The normalized spectrum is

$$\begin{aligned} f(\xi)&=\frac{2(1-\gamma)(2-\gamma)}{\gamma^2}\frac{\xi_0^2}{\xi^3}\left[\left(\frac{\xi}{\xi_0}\right)^{\gamma}-1\right]^2, \qquad \xi_0\leq\xi,\\ f(\xi)&=0, \qquad 0\leq\xi<\xi_0,\\ \gamma&=\tfrac{1}{2}(c+3), \qquad \xi_0=\left(1-\frac{2\gamma}{3}\right)^{1/\gamma}. \end{aligned} \tag{3.20}$$

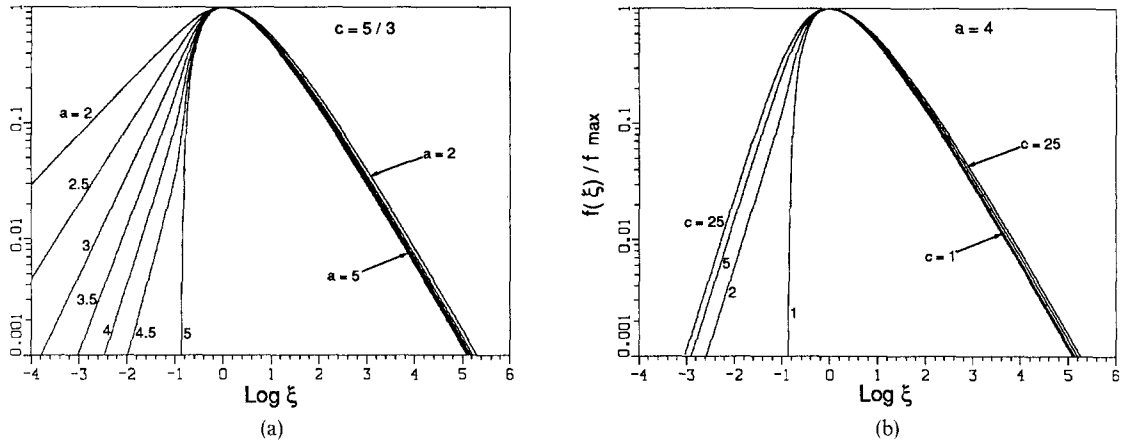

Figure 4. Sensitivity of the homogeneous isotropic spectrum shape in the present model to variations of a and c.

We also have

$$\left(\frac{\beta}{c_2}\right)^2 = 8(1-\gamma)(2-\gamma)\xi_0^2$$

and the self-similar distribution is

$$E_s(k,0;k_0,t_0) = \frac{1}{(c_1+3c_2)^2 t_0^2}\frac{1}{k^3}\left[\left(\frac{k}{k_0}\right)^{\gamma}-1\right]^2, \qquad k_0 \le k. \tag{3.21}$$

If $-3 < c < -\frac{5}{3}$, then $\gamma > 0$ and $f \sim \xi^c$ for $\xi \to \infty$. If $c < -3$, then $\gamma < 0$ and $f \sim \xi^{-3}$ as $\xi \to \infty$.

For $c = -3$, take $\gamma \to 0$ in (3.21) to get

$$f(\xi) = 4\xi_0^2 \xi^{-3} \log^2\left(\frac{\xi}{\xi_0}\right), \qquad \xi_0 \le \xi, \quad \text{with} \quad \xi_0 = e^{-2/3}, \tag{3.22}$$

and

$$E_s(k,0;k_0,t_0) = (2c_2 t_0)^{-2} k^{-3} \log^2\left(\frac{k}{k_0}\right), \qquad k_0 \le k. \tag{3.23}$$

For $t > 0$, $E_s(k,t;k_0,t_0)$ is inferred from (3.21) (note $a = 0$) by the replacements

$$k_0 \to k_0\left(1+\frac{t}{t_0}\right)^{-1}, \qquad t_0 \to t_0 + t.$$

D. Nonzero Viscosity

1. Self-Similar Regimes Including Viscosity. When $\nu > 0$, as we now assume, the viscosity term of the homogeneous isotropic PDE dominates for $k \to \infty$. A self-similar regime including an inertial range may persist up to some wave number $k_d(t)$ to be identified with the Kolmogorov (1941) wave number. The condition is that $\sigma(t)$,

$$\sigma(t) = \frac{\nu k_{\max}(t)}{K(t)^{1/2}}, \tag{3.24}$$

which represents a time-dependent inverse turbulent Reynolds number, be sufficiently small. By Kolmogorov's theory, we should have

$$\xi_d = \frac{k_d(t)}{k_{\max}(t)} \sim (\text{Reynolds number})^{3/4} \sim [\sigma(t)]^{-3/4}. \tag{3.25}$$

As will be seen, the proportionality constant in (3.25) for the spectral transport model is determined by solving an ODE and a qualitative estimate is obtainable without computer aid. For $c > -\frac{5}{3}$, spectrum

shape proportional to (3.17) will be a good fit in the range $k_{\max} < k < k_d$ for the self-similar regime, regardless of the choice of $E(k,0)$. For an inertial range to exist, $\sigma(t)$ must be small enough to allow $k_d/k_{\max} \gg 1$.

Inclusion of the viscous term in the similarity analysis leads to (3.12) as before, but (3.11) is replaced by

$$\frac{d}{d\xi}\left[c_2\xi^{7/2}f^{1/2}\frac{df}{d\xi} - c_1\xi^{5/2}f^{3/2} - \beta\xi f\right] + \alpha f - 2\sigma(t)\xi^2 f = 0, \tag{3.26}$$

where, for $a = 2$,

$$\sigma(t) = \frac{\nu k_{\max}(t)}{K(t)^{1/2}} = \frac{\nu}{K_0^{1/2}L_0} = \text{constant}.$$

Note that the existence of viscosity-included self-similar regimes was recognized earlier (Batchelor, 1953).

Examples of such self-similar solutions to the PDE can be contrived in two ways. First, we can take $E(k,0)$ as a narrowly peaked function leading to a low-k cut-off self-similar distribution. Then a c-value must be chosen to force $a = 2$. In the limit $\nu \to 0$, we have $a \approx \frac{1}{2}(3c+5)$, implying $c \approx -\frac{1}{3}$. For large ν, the appropriate c is found by trial from the ODE. Figures 5(a) and (b) are shape plots for $\nu = \sigma = 10^{-4}$ and 0.1, respectively, made essentially self-similar by setting $c = -\frac{1}{3}$ and $c = -0.52$, respectively. An inertial region exists for $\nu = 10^{-4}$ but not for $\nu = 0.1$.

Second, we can choose c more or less arbitrarily, but force $a = 2$ by choosing $E(k,0)$ proportional to $k(=k^{a-1})$ near $k = 0$. See Figure 5(c) which, with $\nu = \sigma = 0.01$, shows an inertial range of modest size.

2. Overlapping Self-Similar Forms. We now analyze the character of $E(k,t)$ in the dissipation range for large times by a method that applies to arbitrary c and a. We do assume $c > -\frac{5}{3}$ so that "inertial range" refers to a k-dependence of $E(k,t)$ approximating $k^{-5/3}$. A similar method would apply for $c < -\frac{5}{3}$.

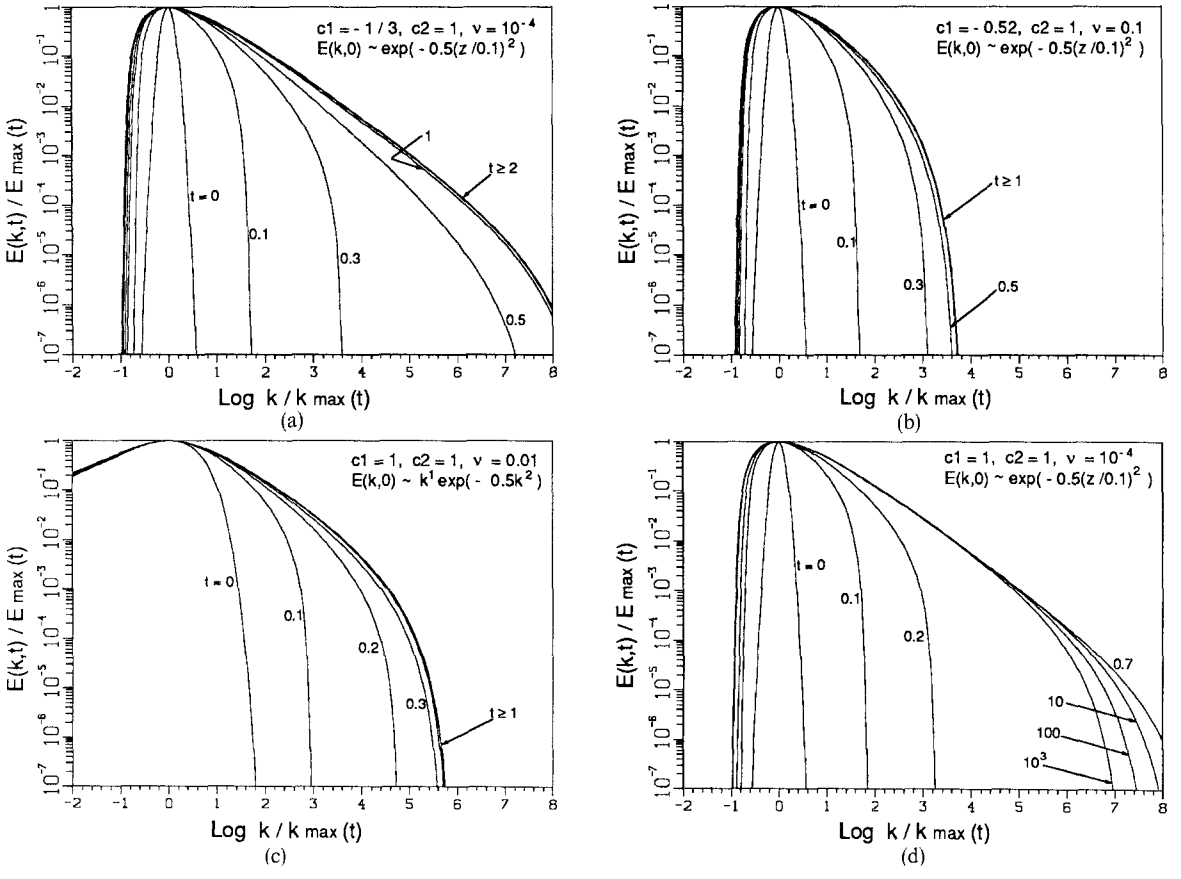

Figure 5. Decays with nonzero viscosity in both self-similar and partially self-similar regimes.

Equation (3.26) is not exact when $\sigma(t)$ is time dependent because f was prescribed as a function of ξ only. If f were generalized to include an additional t dependence, a t-derivative of the new f would have to be included in (3.26).

However, if $\sigma(t)$ is small enough to permit an inertial range, then (3.26) with the σ-term dropped, is still accurate over a *portion* of the spectrum, including the very-large-eddy range ($k \ll k_{\max}$), the dominant-eddy range ($k \approx k_{\max}$), and the inertial range ($k_{\max} < k < k_d$). Equation (3.6) remains valid over this part of the spectrum.

Now, begin again with a new self-similar hypothesis,

$$E(k,t) = \bar{K}(t)\bar{L}(t)\bar{f}(\xi), \qquad \xi = k\bar{L}(t), \tag{3.27}$$

intended to describe the inertial range and the dissipation range, $k > k_d$. A form like (3.9) is again encountered, with an additional term on the right, that is, $-2\nu\xi^2\bar{f}/(\bar{K}^{1/2}\bar{L})$. To reconcile the time dependence of this term with time independence of $\bar{f}$, we assume

$$\frac{\nu}{\bar{K}^{1/2}\bar{L}} = \bar{\sigma} = \text{constant}. \tag{3.28}$$

This would imply that the α- and β-type terms are time dependent, but they are dominated by the transport and viscosity terms in the range of current interest and may be dropped. We are left with

$$\frac{d}{d\xi}\left[c_2\xi^{7/2}\bar{f}^{1/2}\frac{d\bar{f}}{d\xi} - c_1\xi^{5/2}\bar{f}^{3/2} \right] - 2\bar{\sigma}\xi^2\bar{f} = 0. \tag{3.29}$$

Thus, after some relaxation time, $E(k,t)$ is to be described concurrently by two different self-similar forms. The two apply to different, but overlapping, portions of the spectrum. We have not proven that this double self-similarity will evolve from an initial $E(k,0)$, but our numerical experiments validate it.

Because the disregarded α and β terms originated from the $\partial E/\partial t$ term, (3.29) has an additional interpretation. If a steady state is established by, for example, injecting a constant energy source in a localized region of k-space, then (3.29) also describes the equilibrium state outside of that region. Kovasznay (1948) using $c_2 = 0$ and Leith (1967) using $c_1/c_2 = 2$, among others, have applied the equation in that context.

For present purposes we do not need to prescribe normalizations such as (3.7) and (3.8) to make the separation of E in (3.29) into three factors unique. Integration of (3.29) yields

$$\bar{f}(\xi) \to \left(\frac{\bar{\sigma}}{c_2}\right)^2 \frac{\xi}{100}\left(1 - \frac{\xi}{\xi_c}\right)^4 \qquad \text{as} \quad \xi \to \xi_c. \tag{3.30}$$

Numerical integration of (3.29) will establish a relation between the two boundary conditions.

There is one qualification to the above picture. The assumption that the α and β terms are ignorable relative to the retained terms in (3.29) does not apply for $\xi \geq \xi_c$. In a precise calculation of the time evolution with nonzero viscosity, it is found that the behavior predicted by (3.30) is followed until the fall-off from the spectrum maximum is, say, about four or five decades, after which there is a small, exponentially decreasing tail for $\xi \to \infty$.

3. Joining the Self-Similar Solutions. We have shown that, from (3.27) and (3.29), we can extract a solution and a constant $C = C(c)$ such that, in the inertial range,

$$\begin{aligned} E(k,t) &= \bar{K}(t)\bar{L}(t)\left(\frac{\bar{\sigma}}{c_2}\right)^2 C(k_c\bar{L}(t))^{8/3}(k\bar{L}(t))^{-5/3} \\ &= C\left(\frac{\nu}{c_2}\right)^2 k_c^{8/3}k^{-5/3}. \end{aligned}$$

Here, $k_c = k_c(t)$ is the cut-off wave number at the right end of the dissipation range, and the dependences on $\bar{K}, \bar{L}$ have canceled. From (3.6) and (3.11), however, we have, in the inertial range,

$$E(k,t) = K(t)L(t)(kL(t))^{-5/3}f_\infty, \qquad L(t) = \frac{1}{k_{\max}(t)}.$$

Equating the two, we obtain a condition determining the dissipation cutoff in the double self-similar regime:

$$\left(\frac{k_c(t)}{k_{\max}(t)}\right)^{8/3} = \left(\frac{c_2}{\sigma(t)}\right)^2 \left(\frac{f_\infty}{C}\right). \tag{3.31}$$

This still depends on $\sigma(t)$ being sufficiently small. The time dependence of $k_c(t)$ follows from the dependences of $k_{\max}$ and σ, which are known when a is known, and f_∞, C are constants depending on a and c and determined from integrations of ODEs.

Figure 5(d) shows a shape plot for $c_1 = c_2 = 1$, $\nu = 10^{-4}$, and $E(k, 0)$ is a narrow Gaussian, normalized to $\int E(k, 0)\, dk = 1$. The inertial range, established by $t = 0.7$, shrinks slowly as a function of time.

E. Convergence to Self-Similarity

At $t = 0$, let $E(k, t)$ be expressed as

$$E = E_s + \Delta E,$$

where E_s is the self-similar solution to the homogeneous isotropic PDE to which E converges in time. Assume $\Delta E/E_s$ is "not too large," and make the approximation

$$E^{3/2} \to E_s^{3/2} + \tfrac{3}{2} E_s^{1/2} \Delta E. \tag{3.32}$$

For example, the relative error of (3.32) is less than 15% if $-0.39 < \Delta E/E_s < 1$. This leads to a linear equation for ΔE:

$$\frac{\partial}{\partial t}\Delta E = -2\nu k^2 \Delta E - \tfrac{3}{2} c_1 \frac{\partial}{\partial k}(k^{5/2} E_s^{1/2} \Delta E) + c_2 \frac{\partial}{\partial k} k^{7/2} \frac{\partial}{\partial k}(E_s^{1/2} \Delta E). \tag{3.33}$$

We solve (3.33) for $c > -\frac{5}{3}$, $\nu = 0$, and choose (3.18) and (3.19) to represent E_s.

Some lengthy algebra (Besnard *et al.*, 1990) shows that

$$E(k, 0) = E_s(k, 0; k_0, t_0) + k^{-3} x^{-2} (1 - x) \sum_{n=2}^{\infty} C_n P_n(x), \qquad x = \left(\frac{k_0}{k}\right)^{2/3},$$

where the P_n's are Jacobi polynomials. For $t > 0$, put $\lambda_n = 2 + n + 4n(n-1)/9(c+3)$; then

$$E(k, t) = E_s(k, t; k_0, t_0) + k^{-3} x^{-2} (1 - x) \sum_{n=2}^{\infty} C_n \left(1 + \frac{t}{t_0}\right)^{-\lambda_n} P_n(x), \qquad x = \left(\frac{k_0(t)}{k}\right)^{2/3}. \tag{3.34}$$

The condition determining k_0 reduces to

$$\frac{\int E(k, 0) k^{-a} (k_0/k)^{2/3}\, dk}{\int E(k, 0) k^{-a}\, dk} = \frac{p+1}{p+4}, \qquad \text{with} \quad p = \frac{9c + 15}{4}. \tag{3.35}$$

Let $k_{\min}$ be the smallest wave number for which $E(k, 0) \neq 0$. We assume $k_{\min} > 0$, and ask whether

$$\frac{\int E(k, 0) k^{-a} (k_{\min}/k)^{2/3}\, dk}{\int E(k, 0) k^{-a}\, dk} \geq \frac{p+1}{p+4}. \tag{3.36}$$

If (3.36) is valid, (3.55) will place k_0 in the interval $0 < k_0 \leq k_{\min}$.

Equation (3.34) describes the convergence of a cut-off distribution E to a cut-off self-similar distribution E_s and is approximately valid provided that E, E_s, and the residual $\Delta E = E - E_s$ do not violate the approximation (3.32) grossly. Equation (3.36) is a necessary part of this condition. (The analysis for low-k power-law distributions is *much* harder.)

For $t \gg t_0$ and for fixed ratio $k/k_0(t)$, $k^3 E_s$ decreases like t^{-2}. When the approximating condition is adequately satisfied, (3.34) shows that the residual terms decrease like $t^{-\lambda_n}$, with $n \geq 2$. The residual as a whole decreases faster than t^{-4}.

F. A Comparison with EDQNM

From a fundamental standpoint, energy transport in k-space is nonlocal; $\partial E(k)/\partial t$ is determined by values of $E(k')$ not only for k' in the immediate neighborhood of k, but in some larger range. It may be asked to

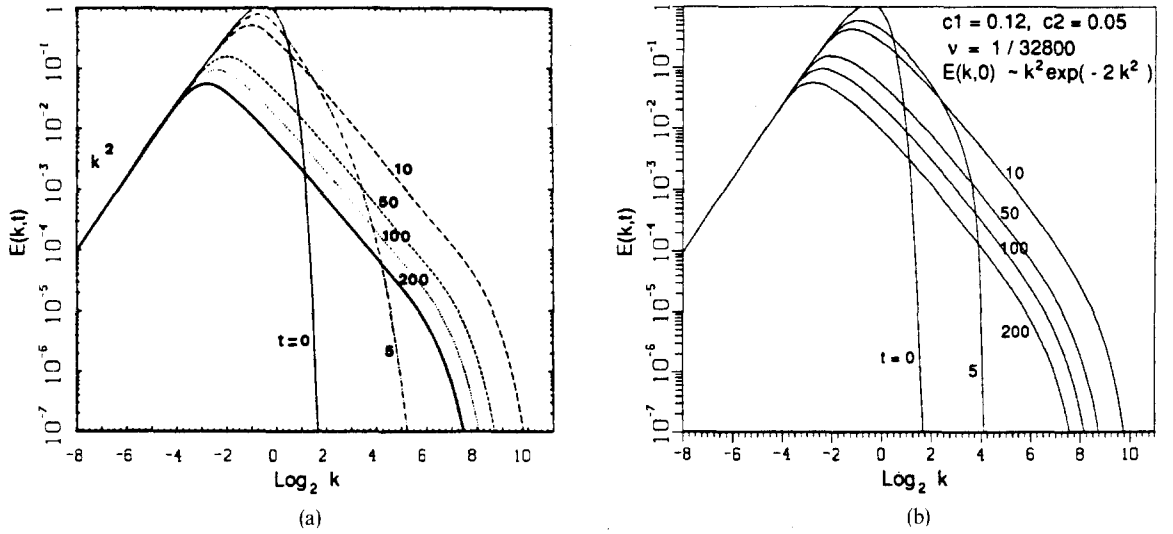

Figure 6. An EDQNM calculation by Lesieur and Schertzer (1978) of a homogeneous isotropic turbulent decay. (b) A calculation in the present model with the same initial conditions and viscosity, and with parameters chosen to match the data of Figure 6(a) at large times.

what extent a phenomenological theory like the present one, which describes k-transport in local terms, can simulate nonlocal phenomena. A simple expedient is to compare it with an explicitly nonlocal theory.

Lesieur and Schertzer (1978) have made a detailed study of the predictions of the (nonlocal) EDQNM model for the decay of homogeneous isotropic turbulence. Figure 6(a) is an evolution plot from Lesieur and Schertzer (1978) copied with permission from the *Journal de Mécanique*, with an initial distribution $E(k,0) \sim k^2 e^{[-k/k_{\max}(0)]^2}$ and an initial turbulent Reynolds number

$$Re = \frac{[\int E(k,0)\,dk]^{1/2}}{\nu k_{\max}(0)} = 32800.$$

Figure 6(b) is the plot for the same initial data and the present model. For this plot, we chose $c_1 = 0.12$, $c_2 = 0.05$ to optimize agreement with the Lesieur–Schertzer curves for $t \geq 10$. Because the objective here is merely to show that local theory can match results of nonlocal theory, there is no implication that these values of c_1, c_2, or of the resultant ratio $c = 2.4$ are optimal for comparison to experiment. Agreement in the approach to self-similarity is not to be expected; in EDQNM $t = 0$ is a time at which triple correlations are assumed to vanish, and relaxation to self-similarity is not a time-translation invariant process. However, for the curves at $t = 10$, 50, 100, 200, the two methods give remarkably similar results.

Lesieur and Schertzer identity a k^4 driving term in the evolution equation for $k \to 0$. Neither the presence of this term in EDQNM nor its absence in (3.1) has a visible effect in Figures 6(a) and (b) because the initial k^2 behavior dominates.

Each curve in Figure 6(b) must cut off at the high-k end with a behavior $\sim (k_c - k)^4$, as we found earlier. Presumably, nonlocality precludes abrupt behavior in EDQNM; but we note that the curves in the dissipation region in the two examples are quite similar even though a range of two to three decades of E values is displayed in that region.

Lesieur and Schertzer also report that if the turbulence has, as an initial condition, a low wave-number spectral behavior of the form $E_{nn}(k, t_0) \approx k^n$, $1 \leq n < 4$, then the low wave-number spectrum is preserved, and the turbulent kinetic energy decays in time as $t^{-\gamma}$, there $\gamma = (2n+2)/(n+3)$. If $n = 4$, corresponding to the Loitsianski integral invariance case, Lesieur and Schertzer indicate that the EDQNM model yields $\gamma = 1.37$, which disagrees with the analyses of Kolmogorov (1941) and of Comte-Bellot and Corrsin (1966). The value of $\gamma = 1.33$ arrived at by Yakhot and Orszag (1986) using the RNG approach, corresponds well with the EDQNM prediction for a value of $n = 3$.

If n is initially greater than 4, Lesieur and Schertzer note that nonlocal interactions in k-space tend to drive the low wave-number spectrum power law to a value of $n = 4$. Our model shows that the low

wave-number power law persists provided than $n+1<\frac{1}{2}(3c+5)$. At large times, the energy decay like $t^{-\gamma}$, $\gamma=(2n+2)/(n+3)$, is in agreement with the EDQNM model for $1\le n<4$.

If the low wave-number cut-off is attained, i.e., if $n+1\ge\frac{1}{2}(3c+5)$, then $\gamma=(2c+10/3)/(c+3)$. Note that if $c>\frac{5}{3}$, then the decay rates observed by Lesieur and Schertzer are also given by our model for $1\le n<4$. This agreement is perhaps due to the fact that if the turbulent field possesses a low wave-number power law with $n<4$, then the contributions to small wave numbers due to triad interactions (which contribute energy at small wave numbers in a manner proportional to k^4) become vanishingly small compared with the energy already present in the region near $k=0$. It is worthwhile noting that the decay law exponent $\gamma=1.3$, as determined by Mohamed and LaRue (1990), corresponds to a power-law exponent of approximately $n=3$ in the model of Leith (1967), our model, and the EDQNM model. This implies that the effect of energy transfer to large scales due to triad interactions is a small effect in grid-generated turbulence and perhaps also in other real turbulent fields.

Note that, for $n=4$, our model disagrees with the EDQNM model, but agrees with Kolmogorov (1941) and Comte-Bellot and Corrsin (1966). For $n>4$, the threshold between persistence of a power law and appearance of a cut-off spectrum depends on the value of c.

In summary, we note that the relations of self-similarity as set forth in Lesieur and Schertzer coincide with the corresponding relations of our model in the limit $t\gg t_0$, i.e., for relaxation times large compared with $K^{-1/2}/k_{\max}$, which represents the cycle time of the dominant eddies. These comparisons support the view that the homogeneous isotropic PDE of our model can simulate turbulence effectively despite its purely local character.

G. Comparison with a Model of Bell and Nelkin

Bell and Nelkin (1978) studied a "cascade model" whose dynamical variables depend on aggregate turbulent kinetic energies in discrete wave-number shells. The nth shell is centered at $k_n=2^n k_0$, or, more generally, at $k_n=h^n k_0$. This paper, which we call BN, was based on earlier work by Bell and Nelkin (1977) and generalizes the model of Desniansky and Novikov (1974a, 1974b). Their model equation is

$$\frac{du_n}{dt}=\alpha k_n(u_{n-1}^2-hu_nu_{n+1})-\alpha k_n h^{-1/3}C(u_{n-1}u_n-hu_n^2)-\nu k_n^2u_n,$$

where

$$\tfrac{1}{2}u_n^2\equiv\tfrac{1}{2}u^2(k_n,t)=\int_{h^{-1/2}k_n}^{h^{1/2}k_n}E(k,t)\,dk.$$

To draw comparisons, we first remark that, for purposes of numerical computation, we utilized variables $\hat{E}(k,t)=kE(k,t)$ and $z=\log k$, so that $E\,dk=\hat{E}\,dz$. Our PDE takes the form

$$\frac{\partial\hat{E}}{\partial t}=-2\nu k^2\hat{E}+\frac{\partial}{\partial z}\left\{-(c_1+c_2)k\hat{E}^{3/2}+c_2k\hat{E}^{1/2}\frac{\partial\hat{E}}{\partial z}\right\}. \tag{3.37}$$

Computations were done by finite differences on a z-mesh with constant mesh spacing Δz.

The BN equation can be re-expressed as

$$\frac{d}{dt}(\tfrac{1}{2}u_n^2)=-2\nu k_n^2(\tfrac{1}{2}u_n^2)-\Delta\{\alpha k_nu_nu_{n-1}^2-\alpha Ck_nu_n^2u_{n-1}\}, \tag{3.38}$$

where we apply the finite difference notation $\Delta F_n=F_{n+1}-F_n$, and make the correspondence $h=e^{\Delta z}$. It is clear that (3.38) is a finite-difference approximation to (3.37) in z-space. In our numerics, most data were about two-figure accurate with mesh spacing of $\Delta z=0.1$ to 0.2. Because BN focused on $\Delta z=\log 2=0.69$, their results should be qualitatively, but not precisely, equivalent to ours.

Following the appendix of BN, we set $C=h^{\zeta/2}$ and compute the limit of (3.38) as $\Delta z\to 0$. To leading order in Δz, the result is (3.37) with

$$c_2=\lim_{\Delta z\to 0}\sqrt{2}(\Delta z)^{-5/2}\alpha,$$

$$\frac{c_1}{c_2}=-\tfrac{5}{3}-\zeta.$$

A key result of BN is that E goes like $k^{-5/3}$ or $k^{-5.3-\zeta}$ in the inertial range, according to whether ζ is negative or positive. This matches exactly our result, which depended on the sign of $c+\frac{5}{3}$.

Lastly, BN noted that Leith's shape functions had a range of power-law behaviors as $k\to 0$ and a range of time-decay laws, and suggested that Leith's equation may have another type of solution with a sharp low-k cut-off, because the BN solutions had a similar character. We have confirmed this and given the cut-off solution explicitly in Section 3.C. In return we can suggest that the BN model also has a range of self-similar power-law solutions; BN could have found them as the long-time limit of a calculation starting from a power law at $t=0$.

4. Free Shear Flow

A. Differential Equations

Consider the flow (Kelvin–Helmholtz instability) of a three-dimensional, incompressible fluid with mean flow along x and mean-flow gradient along y. Assume $u_1(y,t)\to u_\infty=\text{constant}$ as $y\to\infty$, $u_1(-y,t)=-u_1(y,t)$, and $u_1(0,t)=0$. Also, $u_1(y,t)>0$ for $y>0$ and $u_\infty>0$. At $t=0$, we take $|u_1|$ substantially equal to u_∞ for all y, except for a smooth transition from $-u_\infty$ to u_∞, confined to a narrow interval about $y=0$.

We write $\partial u_1(y,t)/\partial y=u_{12}(y,t)$. This is the only nonzero component of mean-flow gradient. The mean pressure $p(y,t)$ is symmetric in y and approaches a constant p_∞ as $y\to\pm\infty$.

This system is studied here for rather limited purposes: to give a comparatively simple example of a calculation for an inhomogeneous flow yielding physically sensible results, to illustrate certain scaling and self-similarity properties that may occur in inhomogeneous flows, and thereby to provide motivation for certain assumptions in the K–ε derivation of the next section.

A more complete analysis, including experimental comparison, will appear in forthcoming papers with Timothy Clark and with Robert Gore.

The evolution equations for E_{ij} couple four linear combinations of the tensor components; these codetermine one another and must be solved for concurrently. These are conveniently taken as $E(y,k,t)$, $\tilde{E}_{11}(y,k,t)$, $\tilde{E}_{22}(y,k,t)$, and $E_{12}(y,k,t)(=\tilde{E}_{12})$. The operators $\mathbf{V}$ and $\mathbf{T}$ of (2.19) become

$$\mathbf{V}=\nu\left(-2k^2+\frac{1}{2}\frac{\partial^2}{dy^2}\right),$$

$$\mathbf{T}=c_D\frac{\partial}{\partial y}\nu_T\frac{\partial}{\partial y}-c_1\frac{\partial}{\partial k}k^2\sqrt{kE}+c_2\frac{\partial}{\partial k}k^3\sqrt{kE}\frac{\partial}{\partial k},$$

where

$$\nu_T\equiv\nu_T(y,t)=\int_0^\infty\sqrt{kE(y,k,t)}\frac{dk}{k^2}.$$

It follows from (2.20) that

$$\frac{\partial E}{\partial t}=\mathbf{V}[E]+\mathbf{T}[E]-2u_{12}E_{12}+3c_{F2}u_{12}\frac{\partial(k\tilde{E}_{12})}{\partial k}, \tag{4.1a}$$

$$\frac{\partial\tilde{E}_{11}}{\partial t}=\mathbf{V}[\tilde{E}_{11}]+\mathbf{T}[\tilde{E}_{11}]-\tfrac{4}{3}(1-c_B)u_{12}E_{12}-\tfrac{2}{3}c_{B1}u_{12}\tilde{E}_{12}+\tfrac{2}{3}c_Fu_{12}\frac{\partial(k\tilde{E}_{12})}{\partial k}-c_Mk\sqrt{kE}\tilde{E}_{11}, \tag{4.1b}$$

$$\frac{\partial\tilde{E}_{22}}{\partial t}=\mathbf{V}[\tilde{E}_{22}]+\mathbf{T}[\tilde{E}_{22}]+\tfrac{2}{3}(1-c_B)u_{12}E_{12}+\tfrac{4}{3}c_{B1}u_{12}\tilde{E}_{12}+\tfrac{2}{3}c_Fu_{12}\frac{\partial(k\tilde{E}_{12})}{\partial k}-c_Mk\sqrt{kE}\tilde{E}_{22}, \tag{4.1c}$$

$$\frac{\partial\tilde{E}_{12}}{\partial t}=\mathbf{V}[\tilde{E}_{12}]+\mathbf{T}[\tilde{E}_{12}]-\tfrac{2}{15}u_{12}E+c_{B1}u_{12}\tilde{E}_{11}-(1-c_B)u_{12}\tilde{E}_{22}+c_Fu_{12}\frac{\partial}{\partial k}(k\tilde{E}_{11}+k\tilde{E}_{22})$$
$$-\tfrac{1}{30}u_{12}\frac{\partial(kE)}{\partial k}-c_Mk\sqrt{kE}\tilde{E}_{12}, \tag{4.1d}$$

In this formulation, $u_1(y)$ is antisymmetric in y, and $u_{12}, E, \tilde{E}_{11}, \tilde{E}_{22}, E_{12}$ are symmetric in y. The E_{ij} and u_{12} vanish at $y \to \pm\infty$. The x-component of the mean-flow equation, (2.6), differentiated with respect to y, yields

$$\frac{\partial}{\partial t}u_{12} = \nu\frac{\partial^2}{\partial y^2}u_{12} - 2\frac{\partial^2}{\partial y^2}\int_0^\infty E_{12}(y,k,t)\,dk. \tag{4.2}$$

Equations (4.1) and (4.2) are now a complete set of coupled equations that determine the evolution of $E, \tilde{E}_{11}$, $\tilde{E}_{22}$, $\tilde{E}_{12}$, and u_{12} for $t > 0$ from their initial values.

Integration of (2.6) over y yields the mean pressure:

$$\frac{p(y)}{\rho} = \frac{p_\infty}{\rho} - 2\int_0^\infty E_{22}(y,k,t)\,dk. \tag{4.3}$$

The remaining components, E_{23} and E_{31}, couple only to each other. For present purposes, we assume $E_{23} = E_{31} = 0$ for $t = 0$, and hence for all $t > 0$.

B. Some Similarities

Turbulence in free shear flow contains at least as many regularities as were displayed above for homogeneous isotropic turbulence. We do not attempt a complete treatment here, but take a first step. We take $\nu = 0$ and look for solutions depending on y and k through the dimensionless combinations η and ζ:

$$\eta = \frac{y}{u_\infty(t+t_0)}, \qquad \zeta = ku_\infty(t+t_0). \tag{4.4}$$

Assume that the tensor functions can be expressed in terms of dimensionless functions of η and ζ:

$$E(y,k,t) = \left(\frac{u_\infty^2}{k}\right)\hat{E}(\eta,\zeta), \tag{4.5a}$$

$$\tilde{E}_{ij}(y,k,t) = \left(\frac{u_\infty^2}{k}\right)\hat{E}_{ij}(\eta,\zeta). \tag{4.5b}$$

For the mean flow, set $u_1(y,t) = u_\infty\hat{u}(\eta)$. In terms of

$$\hat{K}_{12}(\eta) = u_\infty^{-2}\int_0^\infty E_{12}(y,k,t)\,dk = \int\hat{E}_{12}(\eta,\zeta)\frac{d\zeta}{\zeta},$$

the mean-flow equation becomes

$$\eta\frac{\partial\hat{u}}{\partial\eta} = -2\frac{\partial\hat{K}_{12}}{\partial\eta}. \tag{4.6}$$

Hence,

$$u_{12}(y,t) = \frac{1}{t+t_0}\frac{\partial\hat{u}}{\partial\eta} = \frac{2}{\eta(t+t_0)}\frac{\partial\hat{K}_{12}}{\partial\eta}. \tag{4.7}$$

It is now straightforward to verify that the equations for $\hat{E}(\eta,\zeta)$, $\hat{E}_{11}(\eta,\zeta)$, $\hat{E}_{22}(\eta,\zeta)$, and $\hat{E}_{12}(\eta,\zeta)$ constitute a closed system whose solutions, if they exist, represent a self-similar regime. In order to test computations for convergence to, and consistency with, this self-similar regime, we consider some of its implications.

Let $k_{\max}(y,t)$ be the wave number at which $E(y,k,t)$ reaches its maximum, $E_{\max}(y,t)$, for fixed y,t. Let $k_{\max}(t) \equiv k_{\max}(0,t)$, $E_{\max}(t) \equiv E_{\max}(0,t)$.

Next, assume the forms (4.5) are valid, and let $\zeta_{\max}(\eta)$ be the ζ value for which $\hat{E}(\eta,\zeta)/\zeta$ is a maximum. By (4.4), we have

$$\zeta_{\max}(\eta) = u_\infty(t+t_0)k_{\max}(y,t), \tag{4.8a}$$

and, in particular,

$$\zeta_{\max}(0) = u_\infty(t+t_0)k_{\max}(t). \tag{4.8b}$$

Then $1/k_{\max}(t)$ is a linear function of t in the self-similar regime, and its t-intercept identifies t_0. Further, $1/k_{\max}(y,t)$, as a function of t for a fixed value of $\eta = y/u_\infty(t_0+t)$, is linear in t. The definitions (4.4) can now be rewritten:

$$\eta = \frac{yk_{\max}(t)}{\zeta_{\max}(0)}, \tag{4.9a}$$

$$\zeta = \left(\frac{k}{k_{\max}(t)}\right)\zeta_{\max}(0). \tag{4.9b}$$

Thus, up to a constant, η and ζ can be inferred from computed data at time t without prior knowledge of t_0, which requires data at a range of times. It follows that

$$\frac{E(y,k,t)}{E_{\max}(t)} = \frac{\hat{E}(\eta,\zeta)/\zeta}{max_\zeta(\hat{E}/\zeta)} = \text{function only of } yk_{\max}(t) \text{ and } \frac{k}{k_{\max}(t)}. \tag{4.10}$$

C. Numerical Results

Our numerical calculations are surveyed here in graphical form, including some checks on the scaled relations of the previous subsection. Some additional features of similarity, not specifically implied by the previous similarity equations, are also noted. They lead us to approximate self-similarity statement for the general Reynolds tensor in $(\mathbf{x}, k)$-space, which is the point of departure in the next section for a derivation of the K–ε model.

We present data on the numerical solution of (4.1) and (4.2) with $c_2 = 0.148$, $c_1 = 2c_2$, $c_M = 26c_2/9$, $c_B = \frac{16}{21}$, $c_D = 0.05$, and $\nu = 0$. All five of the dimensionless parameters enter into this calculation. The values

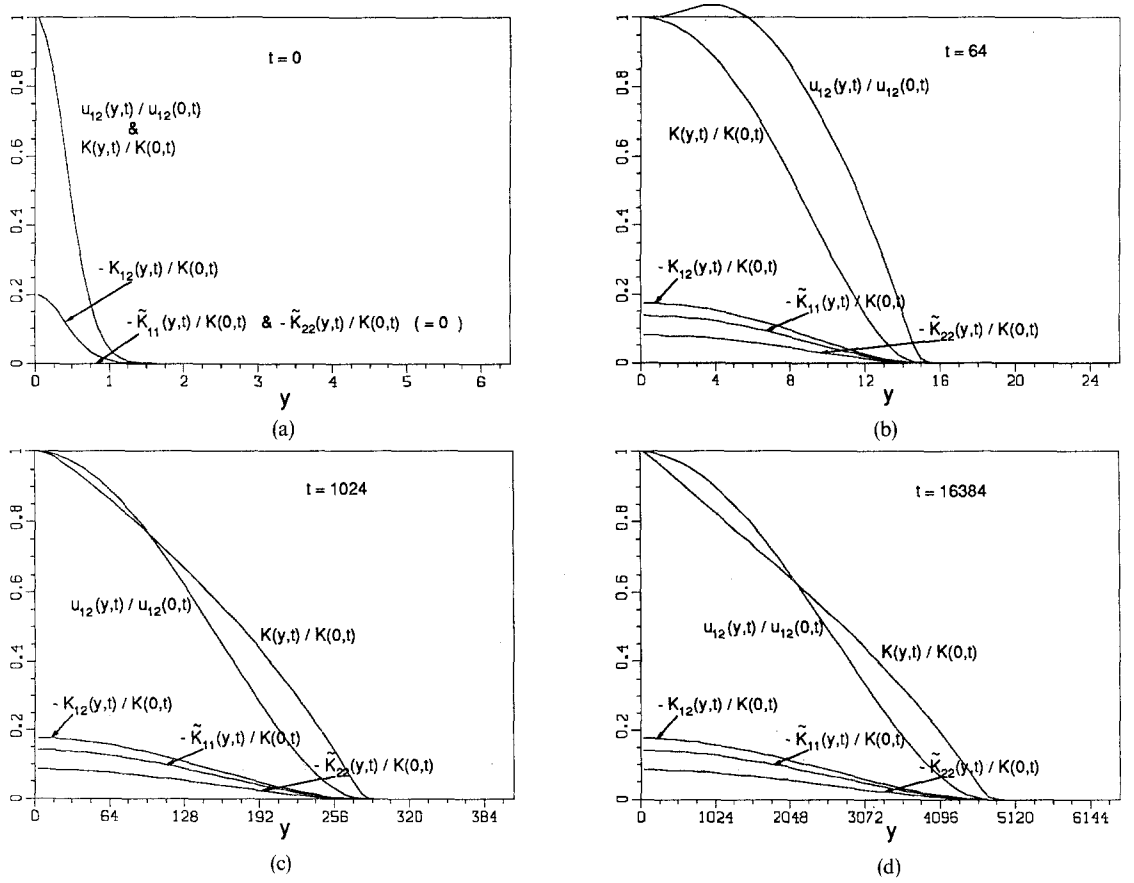

Figure 7. Dependence of mean-flow gradient and Reynolds stress-tensor components on distance from the shear plane and time, in an evolution of free shear flow.

of c_1, c_2 are consistent with the considerations of Section 3.A including $C_K = 1.5$, and the values of c_B and c_M are consistent with estimates of Clark and Zemach (1991) matching experiments on homogeneous flows. The c_D value was set to make the diffusion rate in y-space of the E_{ij} comparable with the diffusion rate of u_{12}. No claim is made at the present time that these illustrative values are best fits to experiment. Initial conditions are chosen that concentrate the k-spectrum about $k = 1$, and concentrate the y-dependence of the functions about $y = 0$. Also, we set $u_\infty = 1$ and $\int E\, dy\, dk = 1$ at $t = 0$.

Figure 7 shows the dependence on the distance y from the shear plane of the mean-velocity gradient $u_{12}(y,t)$, the turbulent energy density $K(y,t) = \int E(k,y,t)\, dk$, and the anisotropic densities $\tilde{K}_{ij}(y,t) = \int \tilde{E}_{ij}(k,y,t)\, dk$ and shows how they diffuse in time. Note that $\tilde{K}_{11}$, $\tilde{K}_{22}$, and $\tilde{K}_{12}$ are negative. (The components of the K tensor are half the components of the Reynolds stress tensor.)

The one feature of regularity, which is critical for the argument of Section 5, is that after a certain relaxation time (in this example, for $t \geq 64$) spectral shapes may become substantially independent of $\mathbf{x}$. This is shown by the shape plots of Figure 8. The apparently single curve in each plot is a superposition of seven curves for seven distances y from the shear plane in the range $0 \leq y \leq 16$, spanning about eight decades of values for $K(y,t)$. ($\tilde{E}_{11}$ and $\tilde{E}_{12}$ are negative. $\tilde{E}_{22}$ is mostly negative, but slightly positive at low k; hence, the $\tilde{E}_{22}$ scale is in linear, rather than logarithmic units.)

Figure 8 also shows the spectra go like powers for k, for large k. The $k^{-5/3}$ behavior for E follows from the form of $\mathbf{T}[E]$, i.e., it is a consequence of energy balance and dimensional analysis, as in the homogeneous isotropic case. Suppose that $E_{12} \sim k^p$ in the self-similar state for large k. Then

$$\mathbf{T}[E_{12}] - c_M k\sqrt{kE}E_{12} \sim \left[p^2 + (\tfrac{5}{3} - c)p - \left(\tfrac{5}{3}c + \frac{c_M}{c_2}\right)\right] k^{p+2/3}, \qquad k \to \infty. \tag{4.11}$$

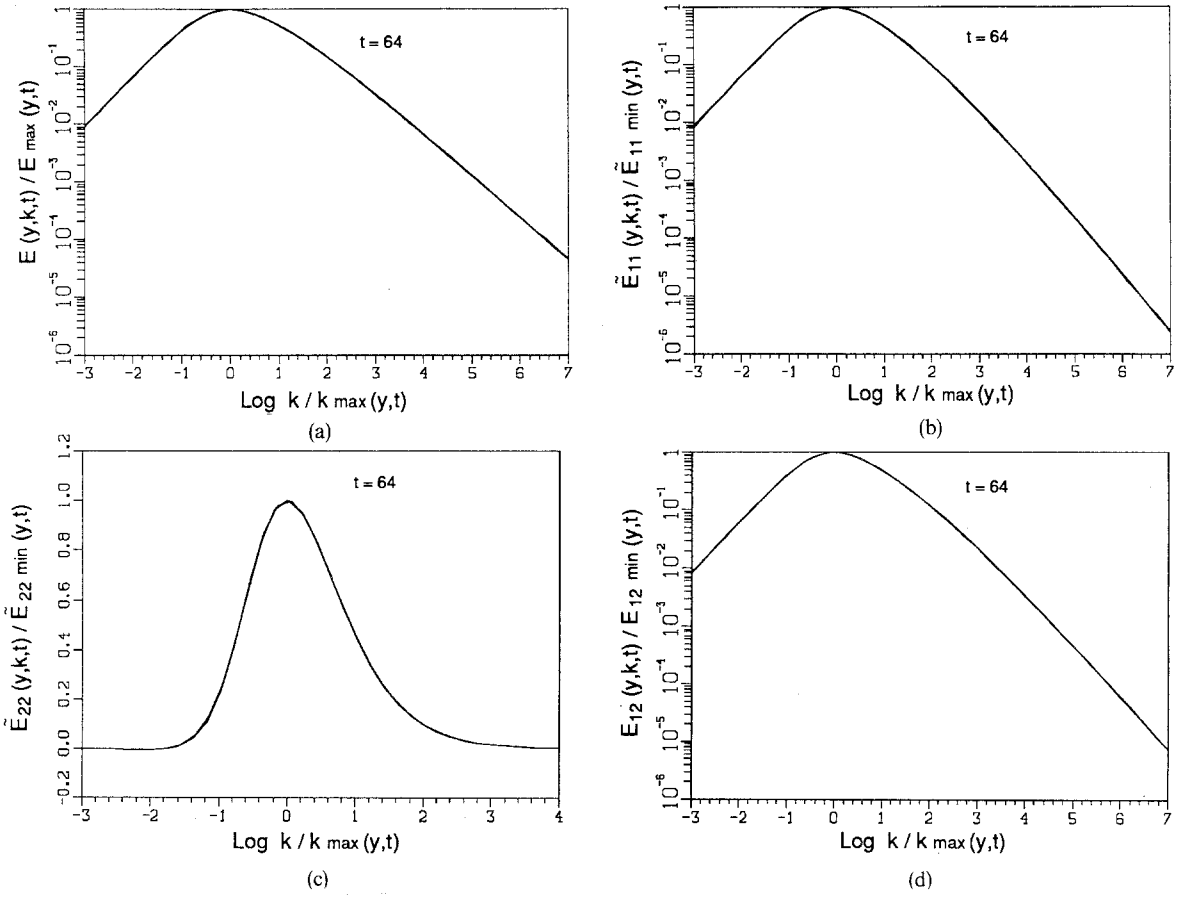

Figure 8. Spectra of energy-tensor components for the flow treated in the text, for $t = 64$, and for seven distances y from the shear plane. The fall-off of turbulent energy density $K(y,t)$ in this range is about eight decades. The seven curves in each plot are nearly coincident, and remain so for $t > 64$.

If E_{12} were some arbitrary distribution in k-space, which was decaying in the *absence* of any mean-flow coupling, then the vanishing of the coefficient of $k^{p+2/3}$ in (4.11) defines an indicial equation in p. Its solution p_0 fixes the leading term k^{p_0} (i.e., the term with least negative exponent) that E_{12} has for large k. We find

$$p_0 = \tfrac{1}{2}(c - \tfrac{5}{3}) - \left[\tfrac{1}{4}(c + \tfrac{5}{3})^2 + \frac{c_M}{c_2} \right]^{1/2}.$$

The negative sign of the square root is taken so that p_0 is negative, and close to $-\frac{5}{3}$ if c_M is close to zero.

For the present case, however, the term in (4.11) may balance off against the $u_{12}E$ term, which implies that $p = -\frac{7}{3}$. If this is the physically realistic case in an experimental situation, as some believe, the implication for our model is that c_M/c_2 be set large enough to make $p_0 \leq -\frac{7}{3}$, and this was done above.

Because the mean-flow coupling in the $d\tilde{E}_{22}/dt$ equation is to E_{12}, but not to E, the same argument gives $\tilde{E}_{11}$ and $\tilde{E}_{22} \sim k^{-9/3}$ in this model. These predictions are consistent with our example for $t \geq 64$.

The data indicate the following paradigm for late times is approximately valid:

$$\textit{each tensor component} = (\text{function of } y, t) \times \text{function of } (k \times \text{function of } y, t).$$

This can be understood as follows. The anisotropic part $\tilde{E}_{ij}$ of the E-tensor is produced by the mean-flow gradient terms and dissipated by the c_M terms. Over time, an equilibrium may be established in, for example, (4.1c) such that

$$\tfrac{2}{15}u_{12}E \approx c_M k\sqrt{kE}E_{12},$$

if the other terms of (4.1c) are relatively unimportant, e.g., for large k. Then the mean-flow term of (4.1a) is like $(u_{12})^2 k^{-3/2}E^{1/2}$. With error of second order in u_{12}, $E(y, k, t)$ can relax to a y-dependent self-similar form $E \approx KLf(\xi)$, $\xi = Lk$. This implies $E_{12} \approx K_{12}L\tilde{f}(\xi)$, with $\tilde{f}(\xi) \sim \xi^{-3/2}f^{1/2}(\xi)$, at least for large k, and $|K_{12}/K| \sim |K^{-12}Lu_{12}| \sim t_0/t_M$.

Here, t_M is the inverse mean-strain rate and is a characteristic time for change of the mean velocity distribution. Assuming that $\frac{1}{2}\alpha + \beta$ in (3.12c) is of the order of unity, t_0 represents both the dominant-eddy cycle time and the waiting time necessary for convergence of a k-distribution to a self-similar form (as in Section 3.F). A condition for approximate self-similarity is then $|K_{12}/K| \ll 1$, or $t_0 \ll t_M$, i.e., deformations of the mean-flow configuration must be slow compared with the periods of the dominant turbulent eddies. The parameters of this numerical example meet these conditions. Other parameters may produce other phenomena; this is a matter for further study.

It is tempting to extrapolate from this example and propose an approximate self-similar form to which a set of general turbulence distributions will converge in time, and which follows the above paradigm. This leads, in the next section, to one-point equations in **x**-space, after some averages over k-space, substantially equivalent to the K–ε equations.

Referring to the complete model equations, (2.22), we expect that $E \sim k^{-5/3}$ for large k in the self-similar state (up to the dissipation region), if such a state is reached, and that $\tilde{E}_{ij} \sim k^{-7/3}$, provided that the E-term in the $\partial\tilde{E}_{ij}/\partial t$ equation that is proportional to $\partial u_i/\partial x_j + \partial u_j/\partial x_i$ does not vanish, and that c_M/c_2 is not too small.

5. Reduction to "One-Point" Equations

We have seen by example and some argument that the late-time solutions of the spectral transport model may be self-similar. This supports the idea that simple transport models, such as "K–ε," may be able to describe adequately a large number of different circumstances.

We integrate the evolution equations for E and $\tilde{E}_{ij}$ over dk to get evolution equations for $K = \int E\,dk$ and $\tilde{K}_{ij} = \int \tilde{E}_{ij}\,dk$ in terms of K, $\tilde{K}_{ij}$, $\partial u_i/\partial x_j$, and a length scale L. L may be considered the inverse of the dominant wave number $k_{\max}$ in the E-spectrum. The dissipation rate $\varepsilon = \varepsilon(\mathbf{x}, t)$ will be identified from the $\partial K/\partial t$ equation as proportional to $K^{3/2}/L$.

By integrating the $\partial E/\partial t$ equation over $k^m\,dk$ for suitable m, we get an equation relating $\partial K/\partial t$ and $\partial L/\partial t$, allowing elimination of L in favor of ε. The Boussinesq approximation is then invoked to express $\tilde{K}_{ij}$ in terms of the other data. This, together with the mean-flow equation, closes the system, and yields the desired reduction to a one-point model similar to a K–ε model.

The result depends on constants related to the five parameters of the spectral transport model, and to moments of the form factors of the E and $\tilde{E}_{ij}$ distributions. As a rough guide to estimating them, we might assume that the form factor for E obeys the homogeneous isotropic ODE, (3.11), which fixed $f(\xi)$ in terms of parameters c and a.

The K–ε model is not a perfect match to experience and neither are our self-similar forms. Our purpose is not to prove the K–ε model, but to clarify the basis for its approximate validity, and to suggest that the spectral transport model can provide improvements.

A. Organizing Assumptions

1. The Self-Similar Forms. The turbulent system is assumed to have relaxed to

$$E(\mathbf{x}, t) = K(\mathbf{x}, t)L(\mathbf{x}, t)f(kL(\mathbf{x}, t)), \tag{5.1a}$$

$$\tilde{E}_{ij}(\mathbf{x}, t) = \tilde{K}_{ij}(\mathbf{x}, t)L(\mathbf{x}, t)\tilde{f}(kL(\mathbf{x}, t)). \tag{5.1b}$$

A more general hypothesis is $\tilde{E}_{ij} = KL\tilde{f}_{ij}$ with the shape functions carrying the indices. This would not lead to the usual form of the K–ε model, and we do not pursue it here. The form factors are normalized to

$$\int f(\xi)\,d\xi = \int \tilde{f}(\xi)\,d\xi = 1, \qquad \xi_{\max} = k_{\max}(\mathbf{x}, t)L(\mathbf{x}, t) = 1,$$

where $\xi = \xi_{\max}$ maximizes $f(\xi)$. Their asymptotic behaviors (see the end of last section) are

$$f(\xi) = f_\infty \xi^{-5/3} + O(\xi^{-7/3}), \qquad \tilde{f}(\xi) = O(\xi^{-7/3}) \quad \text{or, at least,} \quad \tilde{f}(\xi) = o(\xi^{-5/3}). \tag{5.2}$$

We utilize the flux $F_f(\xi)$ for $f(\xi)$ as defined in Section 3.D.2. If $f(\xi)$ obeys the homogeneous isotropic ODE, then, taking (3.15) into account,

$$\lim_{\xi\to\infty} F_f(\xi) = \left(c_1 + \frac{5c_2}{3}\right) f_\infty^{3/2} = \alpha. \tag{5.3}$$

For present purposes, we take this as the *definition* of α, regardless of whether $f(\xi)$ obeys the ODE. The corresponding flux limit for $\tilde{E}_{ij}$ is

$$\lim_{\xi\to\infty}\left[c_1\xi^{5/3}f^{1/2}\tilde{f} - c_2\xi^{7/2}f^{1/2}\frac{d\tilde{f}}{d\xi}\right] = 0.$$

If there are particular components $\partial u_a/\partial x_b + \partial u_b/\partial x_a$ of the strain rate that vanish, two qualifications are needed. First, it might be inappropriate to model $\tilde{E}_{ab}$ with the same form factor $\tilde{f}(\xi)$ as the other $\tilde{E}_{ij}$, because their large-k behaviors are different, as noted in the previous section. In modeling the evolution of the full Reynolds tensor, a large family of form factors might be necessary. However, second, such $\tilde{E}_{ab}$ do not contribute to the mean flow coupling ($\sim \partial u_m/\partial x_n \tilde{E}_{mn}$) in the $\partial E/\partial t$ equation, and hence do not affect the derivation of K–ε that merely substitutes a Boussinesq approximation of $\tilde{E}_{mn}$ in this coupling.

2. Moments. We encounter several types of moments over the f and $\tilde{f}$ distributions. First,

$$I_m = \int \xi^m f(\xi)\,d\xi, \qquad J_m = \int \xi^m \frac{d}{\xi} F_f(\xi)\,d\xi$$

and

$$\tilde{I}_m = \int \xi^m \tilde{f}(\xi)\,d\xi. \tag{5.4}$$

If $f(\xi)$ and $\tilde{f}(\xi) \sim \xi^{a-1}$, $\xi \to 0$, and $f(\xi) \sim \xi^{-5/3}$, $\xi \to \infty$, these moments are well defined for

$$-a < m < \tfrac{2}{3}. \tag{5.5}$$

(There is no lower limit on m if $f(\xi)$ and $\tilde{f}(\xi)$ are cut-off distributions.) When $f(\xi)$ approximates the solution of the homogeneous isotropic ODE, we can take moments of the ODE and estimate that

$$\frac{J_m}{I_m \alpha} = 1 + \frac{m}{a}. \tag{5.6}$$

Next, the turbulent diffusion terms in the spectral transport equations simplify as follows:

$$c_D \frac{\partial}{\partial x_n}\left(v_T(\mathbf{x}) \frac{\partial}{\partial x_n} E_{ij} \right) \to c_D M_D \frac{\partial}{\partial x_n}\left(K^{1/2} L \frac{\partial}{\partial x_n} E_{ij} \right),$$

where

$$M_D = \int \xi^{-3/2} f^{1/2}(\xi)\, d\xi. \tag{5.7}$$

Finally, the k integral of the tensor-mixing term is

$$\int c_M k \sqrt{kE}\, \tilde{E}_{ij}\, dk = \frac{c_M}{L} M_M K^{1/2} \tilde{K}_{ij},$$

where

$$M_M = \int \xi^{3/2} f^{1/2}(\xi) \tilde{f}(\xi)\, d\xi. \tag{5.8}$$

A (crude) estimate is obtained by assuming that in the self-similar limit, the c_M term and the mean-flow terms containing E, (i.e., the C_{ij} terms) dominate in (2.22b). This leads to

$$\tilde{f}(\xi) \approx \frac{\xi^{-3/2} f^{1/2}}{N}, \qquad N = \int \xi^{-3/2} f^{1/2}(\xi)\, d\xi,$$

for the normalized $\tilde{f}$, whence

$$M_M \approx \int \frac{f(\xi)\, d\xi}{N} = \frac{1}{M_D}. \tag{5.9}$$

This expression for $\tilde{f}$ in terms of $f(\xi)$ is not reliable for $\xi \to 0$ where the c_M term would be dominated by transport terms, and we do not use it to estimate $\tilde{I}_m$. Equation (5.9) is to be considered no better than an order-of-magnitude estimate.

3. Inertial Range and Viscosity. The postulated forms for $E, \tilde{E}_{ij}$ can only be valid for k up to some Kolmogorov wave number $k_d(\mathbf{x}, t)$ after which viscous dissipation takes over. The viscosity is now assumed small enough, and the inertial range is assumed broad enough, that the moment integrations, which should only be carried out up to $\xi = \xi_d = k_d L$, are adequately approximated by taking the limit $\xi_d \to \infty$. In a more precise analysis, or one in which ν is not "small enough," ξ_d becomes another parameter of the modeling, and one might have to contend with $\mathbf{x}$- and t-dependence of ξ_d. We ignore this complication. Within the broad, but finite, range of k-space in which the k-integrals are done, viscous dissipation is ignored, and viscous diffusion is ignored relative to turbulent diffusion.

B. The Moment Equations

The forms (5.1) will not, in general, satisfy the evolution equations exactly for any choice of K, L, $\tilde{K}_{ij}$. We seek a best-fit approximation to K, L, $\tilde{K}_{ij}$ by substituting (5.1) into (2.22), and requiring that certain equalities obtained from averages over k be satisfied. We also drop the viscosity terms at this point. First, integrate over dk to get, with $D/Dt = \partial/\partial t + u_l \partial/\partial x_l$,

$$\frac{DK}{Dt} = -2 \frac{\partial u_l}{\partial x_n} \tilde{K}_{ln} - \frac{\alpha K^{3/2}}{L} + c_D M_D \frac{\partial}{\partial x_n}\left(K^{1/2} L \frac{\partial K}{\partial x_n} \right), \tag{5.10a}$$

$$\frac{D\tilde{K}_{ij}}{Dt} = -\tfrac{2}{15}\left(\frac{\partial u_i}{\partial x_j}+\frac{\partial u_j}{\partial x_i}\right)K-(1-c_B)\left(\frac{\partial u_i}{\partial x_n}\tilde{K}_{nj}+\frac{\partial u_j}{\partial x_n}\tilde{K}_{in}-\frac{2\delta_{ij}}{3}\frac{\partial u_n}{\partial x_l}\tilde{K}_{nl}\right)$$
$$+c_{B1}\left(\frac{\partial u_n}{\partial x_i}\tilde{K}_{nj}+\frac{\partial u_n}{\partial x_j}\tilde{K}_{in}-\frac{2\delta_{ij}}{3}\frac{\partial u_n}{\partial x_l}\tilde{K}_{nl}\right)+c_D M_D\frac{\partial}{\partial x_n}\left(K^{1/2}L\frac{\partial \tilde{K}_{ij}}{\partial x_n}\right)-c_M M_M\frac{K^{1/2}}{L}\tilde{K}_{ij}. \quad (5.10b)$$

Second, choosing m in the interval (5.5), integrating (2.22a) over $k^m\,dk$, and dividing by I_m, we have

$$\frac{D}{Dt}\left(\frac{K}{L^m}\right) = -\frac{2\partial u_n}{\partial x_l}\frac{\tilde{I}_m(1-3mc_{F2}/2)}{I_m}\frac{\tilde{K}_{nl}}{L_m}-\frac{J_m K^{3/2}}{I_m L^{m+1}}+c_D M_D\frac{\partial}{\partial x_n}\left(K^{1/2}L\frac{\partial}{\partial x_n}\frac{K}{L^m}\right). \quad (5.10c)$$

The choice of m is discussed below.

From the first of these equations, we infer, for the energy dissipation rate $\varepsilon(\mathbf{x}, t)$,

$$\varepsilon = \frac{\alpha K^{3/2}}{L}. \quad (5.11)$$

To get a $D\varepsilon/Dt$ equation independent of DL/Dt, set

$$\varepsilon = \alpha K^{(3m-2)/2m}\left(\frac{K}{L^m}\right)^{1/m}$$

and take the logarithmic derivative:

$$\frac{D\varepsilon}{Dt} = \frac{\varepsilon}{K}\left[\frac{3m-2}{2m}\frac{DK}{Dt}+\frac{1}{m}L^m\frac{D}{Dt}\left(\frac{K}{L^m}\right)\right]. \quad (5.12)$$

Substituting (5.10a) and (5.10c) into (5.12), eliminating L in the result and in (5.10a) by means of (5.11), we get K–ε equations in their *first form*:

$$\frac{DK}{Dt} = -2\frac{\partial u_l}{\partial x_n}\tilde{K}_{ln}-\varepsilon+g_D\frac{\partial}{\partial x_n}\left(\frac{K^2}{\varepsilon}\frac{\partial K}{\partial x_n}\right), \quad (5.13a)$$

$$\frac{D\varepsilon}{Dt} = -2\frac{\partial u_l}{\partial x_n}\frac{\varepsilon}{K}g_{\varepsilon 1}\tilde{K}_{ln}-g_{\varepsilon 2}\frac{\varepsilon^2}{K}+g_D\frac{\partial}{\partial x_n}\left(\frac{K^2}{\varepsilon}\frac{\partial \varepsilon}{\partial x_n}\right)-\frac{g_D}{3}\left\{\frac{K^2}{\varepsilon^2}\left(\frac{\partial \varepsilon}{\partial x_n}\right)^2+(2-3m)\left(\frac{K}{\varepsilon}\frac{\partial \varepsilon}{\partial x_n}-\frac{3}{2}\frac{\partial K}{\partial x_n}\right)^2\right\}. \quad (5.13b)$$

The new constants $g_{\varepsilon 1}$, $g_{\varepsilon 2}$, g_D are

$$g_{\varepsilon 1} = \frac{3}{2}+\frac{\tilde{I}_m(1-3mc_{F2}/2)-I_m}{(mI_m)}, \quad (5.14a)$$

$$g_{\varepsilon 2} = \frac{3}{2}-\frac{1}{m}+\frac{J}{(m\alpha I_m)}, \quad (5.14b)$$

$$g_D = c_D M_D \alpha = c_D M_D\left(\frac{f_\infty}{c_K}\right)^{3/2}. \quad (5.14c)$$

The derivation of the g_D terms in (5.13b) is outlined in Appendix B; the rest of the algebra is straightforward. Note the alternative form for the g_D terms in (B.3) of Appendix B.

If the self-similar representations were exact, these equations would be independent of m. Their sensitivity to the choice of m is a measure of the imperfection of the K–ε model, as deduced from the spectral transport model. The ratio of mean-flow coupling coefficients in the two equations is 3/2 plus a correction due to the relative differene in the mth moments of $f(\xi)$ and $\tilde{f}(\xi)$. This traces back to a derivative of $\varepsilon\,(=\alpha K^{3/2}/L)$ with respect to K in the derivation.

Whatever the errors in the DK/Dt and $D(K/L^m)/Dt$ terms may be, their contributions to the error in $D\varepsilon/Dt$ are seen to be strongly magnified when m is close to zero. On the other hand, a strongly negative m-value may overemphasize the $k \approx 0$ part of the spectrum. Perhaps, it is reasonable to look for variations in the predictions of this analysis for m-values in the neighborhood of the interval $(-2, -1)$.

If we apply (5.6), the decay-term coefficient in the ε-equation becomes

$$g_{\varepsilon 2} = \frac{3}{2} + \frac{1}{a}. \tag{5.15}$$

One of the g_D terms in (5.13b) is of the familiar diffusion type, while the others are negative definite, augmenting the decay.

C. The Boussinesq Approximation

The c_M terms of (5.10b) would return the K-tensor to isotropy, that is, drive the $\tilde{K}_{ij}$ components to zero, if there were no coupling to mean-flow gradients to sustain them. At late times, assume the evolution reaches an equilibrium with respect to this competition. For such an equilibrium, we have $D\tilde{K}_{ij}/Dt \approx 0$ in (5.10b). Suppose, in addition, that the diffusion term and the mean-flow coupling to $\tilde{K}_{ij}$ in (5.10b) are small compared with the mean-flow coupling to K. (Conditions for this are noted below.) Then the equilibrium is expressed as

$$-\frac{2}{15}\left(\frac{\partial u_i}{\partial x_j} + \frac{\partial u_j}{\partial x_i}\right)K - \frac{c_M M_M}{\alpha}\frac{\varepsilon}{K}\tilde{K}_{ij} = 0.$$

Hence

$$\tilde{K}_{ij} = -g_M \frac{K^2}{2\varepsilon}\left(\frac{\partial u_i}{\partial x_j} + \frac{\partial u_j}{\partial x_i}\right), \tag{5.16}$$

where

$$g_M = \frac{\frac{4}{15}\alpha}{c_M M_M} = \frac{\frac{4}{15}(f_\infty/C_K)^{3/2}}{c_M M_M}. \tag{5.17}$$

The *second form* of our K–ε equations is obtained by substituting (5.16) into (5.13a) and (5.13b):

$$\frac{DK}{Dt} = g_M \frac{K^2}{\varepsilon}\frac{\partial u_l}{\partial x_n}\left(\frac{\partial u_l}{\partial x_n} + \frac{\partial u_n}{\partial x_l}\right) - \varepsilon + g_D \frac{\partial}{\partial x_n}\left(\frac{K^2}{\varepsilon}\frac{\partial K}{\partial x_n}\right), \tag{5.18a}$$

$$\begin{aligned}\frac{D\varepsilon}{Dt} = {} & g_M g_{\varepsilon 1} K \frac{\partial u_l}{\partial x_n}\left(\frac{\partial u_l}{\partial x_n} + \frac{\partial u_n}{\partial x_l}\right) - g_{\varepsilon 2}\frac{\varepsilon^2}{K} + g_D \frac{\partial}{\partial x_n}\left(\frac{K^2}{\varepsilon}\frac{\partial \varepsilon}{\partial x_n}\right) \\ & - \frac{g_D}{3}\left\{\frac{K^2}{\varepsilon^2}\left(\frac{\partial \varepsilon}{\partial x_n}\right)^2 + (2-3m)\left(\frac{K}{\varepsilon}\frac{\partial \varepsilon}{\partial x_n} - \frac{3}{2}\frac{\partial K}{\partial x_n}\right)^2\right\}.\end{aligned} \tag{5.18b}$$

The equations are now closed.

The selection of terms in (5.10b) leading to Boussinesq (5.16) rested on the two inequalities

$$|\tilde{K}_{ij}| \ll K \quad \text{and} \quad \left|\frac{\partial}{\partial x_n} K^{1/2} L \frac{\partial \tilde{K}_{ij}}{\partial x_n}\right| \ll K|\nabla \mathbf{u}|. \tag{5.19}$$

The definitions of the length and time scales discussed earlier can be adapted to the present context:

$L_M \approx$ length scale for variation in $\mathbf{x}$-space of $K(\mathbf{x}, t)$, $L(\mathbf{x}, t)$, and $\mathbf{u}(\mathbf{x}, t)$.

$L_T \approx |L(\mathbf{x}, t)| \approx$ length scale for turbulent fluctuations.

$t_M \approx |\nabla \mathbf{u}(\mathbf{x}, t)|^{-1} \approx$ time scale for change in the mean flow configuration.

$t_0 \approx K^{-1/2} L \approx$ cycle time (turnover time) for the dominant turbulent eddies, and $\approx$ time for establishment of spectral equilibrium.

Equation (5.16) implies that $|\tilde{K}_{ij}/K| \approx t_0/t_M$. The conditions for the inequalities (5.19) become

$$\frac{t_0}{t_M} \ll 1 \quad \text{and} \quad \left(\frac{L_T}{L_M}\right)^2 \ll 1.$$

In summary, there are three basic physical conditions that brought us from the Navier–Stokes equations to a K–ε model: that the turbulent length scale be less than the mean length scale, that changes in the

mean-flow configuration be slow compared with the turnover time of dominant turbulent eddies (to establish both spectral equilibrium and the Boussinesq relation), and that turbulent Reynolds numbers be large enough to permit a significant inertial range. Our spectral transport model rests on the first of these conditions, but not on the second or third. In addition, our model, at least in its simplest form, makes choices based on criteria of simplicity, including averaging over directions in **k**-space; the errors incurred by these choices remain to be clarified.

D. Survey of Parameters in the K–ε Models

The spectral transport model was formulated in terms of five parameters: c_B, c_D, c_M, c_1, and c_2. For comparison with other work, we regard $c_K = (c_1 + 5c_2/3)^{-2/3}$ and $c = c_1/c_2$ as parameters, and the Kolmogorov constant c_K is given its experimental value.

In addition, the homogeneous isotropic self-similar state had a parameter a, related to the initial energy distribution relaxing to that state. For stability, the maximum a-value was $a_{\max} = \frac{1}{2}(3c + 5)$, corresponding to the cut-off distribution given by (3.25). For $a < a_{\max}$, $f(\xi)$ behaved like ξ^{a-1}, and E behaved like k^{a-1} near the wave-number origin. For large t, the turbulent energy of a homogeneous isotropic decaying state goes like $t^{-\gamma_K}$, $\gamma_K = a/(1 + \frac{1}{2}a)$. Letting c range from, say, 0 to 10, and letting a range from $a_{\max}$ down to, say, $a = 2.5$ we find by integration of the homogeneous isotropic ODE that

$$f_\infty \text{ ranges from } \tfrac{10}{9} \approx 1.11 \text{ up to } 1.3,$$
$$f_{\max} \text{ ranges from } \tfrac{160}{729} \approx 0.22 \text{ down to } 0.17, \text{ and}$$
$$M_D \text{ ranges from } (\tfrac{9}{10})^{3/2} \approx 0.85 \text{ up to } 3.0.$$

The reduction to K–ε equations reduces the number of parameters to four: $g_{\varepsilon 1}$, $g_{\varepsilon 2}$, g_D, and g_M. In addition, m may be given a specific value for a best fit.

In Section 2 invariance arguments applied to the pressure–velocity correlation led to mean-flow coupling characterized by coefficients c_B, c_{B1}, c_F, and c_{F2} in (2.22). This structure parallels that of Model 1 in the (one-point) modeling of Launder *et al.* (1975). For simplicity, Model 2 of this reference might be followed which amounts to setting $c_{B1} = c_{B2} = 0$ in (2.20). The only consequence for this section is that in the definition of g_M, (5.17), the factor $\frac{4}{15}$ is replaced by $\frac{2}{3}(1 - c_B)$. The best estimate for Model 2 gives $c_B = 0.6$, so that the factor retains the value $\frac{4}{15}$. Thus, both alternatives have the same effect on the reduction to one-point equations. (There are also additional terms in (5.10b) depending on the $\tilde{K}$ tensor as in Model 1, but which, in the Boussinesq approximation, cause no change to the K–ε equations.)

The only effect of MF' terms on the reduction to one-point equations is the appearance of the factor $(1 - 3mc_{F2}/2)$ multiplying $\tilde{I}_M$ in (5.10c). Proceeding again from the data in Launder *et al.* (1975) $3c_{F2}/2$ is less than 0.01, and may be zero within the uncertainties of the parameter fitting; we ignore this correction here.

In preparation for further estimates, we suppose, for the sake of a rough estimate, that f obeys the homogeneous ODE with an a-value characteristic of the small-k power law in the decay of homogeneous turbulence. It would be interesting to check this in inhomogeneous flows that fit the K–ε model. Warhaft and Lumley (1978), and Warhaft (1980) obtained $\gamma_K = 1.34$ and $\gamma_K = 1.33$, respectively. Comte-Bellot and Corrsin (1966) had previously found $\gamma_K = 1.26$. The renormalization group evaluation of Yakhot and Orszag (1986) gave $\gamma_K = 1.33$. Somewhat arbitrarily, we choose $a = 4$ so that $\gamma_K = \frac{4}{3}$, and choose $c_1/c_2 = 2.0$ and Kolmogorov constant $c_K = 1.5$; $(f_\infty/c_K)^{3/2} = 0.66$, $M_D = 1.23$ and, accepting (5.9), $M_M = 0.82$.

A correspondence is given in Table 1 between the coefficients of the standard K–ε model (see, for example, Bradshaw *et al.*, 1981 and our derivation. The main result is that the overall form of our equations tracks well with the standard model.

We do have additional gradient product terms in the second line of (5.13b) augmenting ε-decay. such terms would not have been foreseen in the K–ε phenomenological derivations. Because of this augmentation, it is reasonable that our ε-decay coefficient $g_{\varepsilon 2}$ be somewhat less than the coefficient $c_{\varepsilon 2}$ of K–ε. Our model implies that the turbulent diffusion coefficients for the K and ε equations are both equal to a single parameter g_D, while the existing theory has differences, corresponding to $\sigma_k = 1$, $\sigma_\varepsilon = 1.3$. It would be interesting to see how inclusion of the grad K and grad ε terms would affect optimization of the parameter fit to experiments.

Table 1. Comparison of K–ε coefficients.

	Standard model	Present derivation
Diffusion of K	$c_\mu/\sigma_k = 0.09$	$g_D = c_D M_D (f_\infty/c_K)^{3/2}$
Diffusion of ε	$c_\mu/\sigma_\varepsilon = 0.07$	g_D
Mean flow coupling to K	$c_\mu = 0.09$	$g_M = \frac{4}{15}(f_\infty/c_K)^{3/2}/(c_M M_M)$
Mean flow coupling to ε	$c_{\varepsilon 1} c_\mu$	$g_{\varepsilon 1} g_M$
	$c_{\varepsilon 1} = 1.45$	$g_{\varepsilon 1} = \frac{3}{2} + (\tilde{I}_m - I_m)/(m I_m)$
Decay of ε	$c_{\varepsilon 2} = 1.9$	$g_{\varepsilon 2} = 1.75$

Taking g_D equal to the average of c_μ/σ_k and $\sigma_\mu/\sigma_\varepsilon$, we get $c_D = 0.10$. From $c_\mu = g_M$, we find $c_M = 2.4$. The value of $g_{\varepsilon 2}$, with the assumption of (5.6) that $f(\xi)$ approximates its homogeneous isotropic value, and with $a = 4$, is estimated from (5.15) at 1.75. This is to be compared with the more established value of $c_{\varepsilon 2} = 1.9$. The agreement of $g_{\varepsilon 1}$ with $c_{\varepsilon 1}$ is good because $g_{\varepsilon 1} = 1.5$ plus a small correction depending on the fractional difference of $\tilde{I}_m$ and I_m. That this correction should amount to $c_{\varepsilon 1} - 1.5 = -0.05$ is not unreasonable. These estimates are crude, of course, but with the exception of the c_M estimate, are not too out of line with the (also tentative) parameter values cited in Section 5 and obtained by Clark and Zemach (1991) by another procedure. They need to be refined by more precise matching of the spectral transport model to data, including data not in spectral equilibrium for which the one-point models are inappropriate.

6. Summary of the Model and Possible Extensions

A set of partial differential equations for the evolution of incompressible turbulent flows in interaction with time- and space-dependent mean velocity fields has been constructed. The dependent variables are the components of the turbulent energy density tensor $E_{ij}(\mathbf{x}, k, t)$. These are defined as Fourier transforms, with respect to the relative variables $\mathbf{x}_1 - \mathbf{x}_2$, of half the two-point velocity-fluctuation correlations $\langle u_i'(\mathbf{x}_1) u_j'(\mathbf{x}_2) \rangle$, which are then shell-averaged over directions of the Fourier transform variable, i.e., the wave vector $\mathbf{k}$. Modeling of turbulent spectra varying with wave number $k = |\mathbf{k}|$ permits specification of turbulent interactions at all length scales, at rates which are functionally dependent on these length scales.

Proceeding from the Navier–Stokes equations, we treat the two-point correlations analytically and model the three-point correlations in terms of their expected physical effects. The qualitative notion that mean length scales generally exceed turbulent length scales—excepting, perhaps, in the very-large-eddy region of the spectra where turbulent interactions are especially weak—is exploited to express turbulence production in terms of mean-velocity gradients, but no higher derivatives of mean velocity appear. Additional assumptions express turbulent diffusion in physical space, cascade in k space, and "return to isotropy" by a rather straightforward extension of ideas embodied in earlier one-point modelings of inhomogeneous turbulence and in earlier spectral modeling of homogeneous isotropic turbulence.

The resulting equations depend on five dimensionless parameters. Preliminary values for them, based on more recent work not reported here, are given in Section 4. The calculations and comparisons of this paper encourage us to believe that the model is soundly based, but much testing and validation remains to be done.

In addition, we can point to three modeling steps arising from the need for some control on the model's complexity in the first stages of exploration, rather than from a physical inference, which are early candidates for improvement. First, the expression of k-cascade by local interactions in k-space could be generalized to, for example,

$$\int d\lambda g(\lambda) \left[k^{3/2} \sqrt{E(k)} E(\lambda k) - \frac{1}{\lambda} \left(\frac{k}{\lambda} \right)^{3/2} \sqrt{E\left(\frac{k}{\lambda} \right)} E(k) \right].$$

This reduces to the local form when the distribution function $g(\lambda)$ is sharply peaked around $\lambda = 1$. Whereas the local form expresses the idea that the aggregate effect of the wave-number triads generated by the Navier–Stokes equations can be represented by nearly equilateral triads, the above form extends the

representation to isosceles triads, which recent numerical simulations suggest would be an important step toward reality. Second, the form assumed for turbulent diffusion was only the simplest among a number of plausible alternatives. Assessment of these alternatives can perhaps best be done by comparison with accurate numerical simulations of the sort now becoming possible, e.g., of the decay of initially inhomogeneous distributions of E_{ij} in the absence of mean-flow gradients. Third, if k-shell averaging is not done, then, at the price of promoting the equations from one-dimensional (real) to three-dimensional (complex) in $\mathbf{k}$-space and opening up additional options for the modeling of k-cascade, the important capability to describe anisotropy in $\mathbf{k}$-space is acquired, and introduction of the c_B-class of coefficients is avoided.

Acknowledgments

We are indebted to Roy Axford and Julian Cole for advice on the application of invariance principles to partial and ordinary differential equations, to Andrew Fedorchek for aid in their numerical solutions, to Greg Pollak and Leaf Turner for helpful advice, and to Timothy Clark and Robert Kraichnan for theoretical and philosophical insights.

Appendix A. Fourier Transforms and Operator Expansions

From representations of the two-point functions in $(\mathbf{x}_1, \mathbf{x}_2)$-space, or equivalently $(\mathbf{x}, \mathbf{r})$-space, we pass by Fourier transform to representations in $(\mathbf{x}, \mathbf{k})$-space, where the wave number $\mathbf{k}$ is the transform variable conjugate to $\mathbf{r}$. The use of Fourier transforms here presupposes that the domain of the $\mathbf{r}$-variable, and hence of space-coordinate variables generally, is the whole of physical space. If the fluid were confined, say, to a half-plane, or between walls, the definition of the spectral functions would have to be adjusted, at least for $\mathbf{x}$-values within L_T of the boundaries. Thus, we write

$$R_{ij}(\mathbf{x}, \mathbf{k}) = \int e^{-i\mathbf{k}\cdot\mathbf{r}} R_{ij}(\mathbf{x}_1, \mathbf{x}_2)\, d\mathbf{r}$$

$$= \int e^{-i\mathbf{k}\cdot\mathbf{r}} \langle u_i'(\mathbf{x} + \tfrac{1}{2}\mathbf{r}) u_j'(\mathbf{x} - \tfrac{1}{2}\mathbf{r}) \rangle\, d\mathbf{r}. \tag{A.1}$$

The other terms in (2.2) can be similarly transformed to yield $A_{ij}(\mathbf{x}, \mathbf{k})$, $\Pi_j(\mathbf{x}, \mathbf{k})$, $T_{inj}(\mathbf{x}, \mathbf{k})$, etc. Note that the same symbol is used for the function in its $\mathbf{x}_1, \mathbf{x}_2$ and $\mathbf{x}, \mathbf{k}$ representations; this limits the proliferation of notation and should not lead to confusion.

The $R_{ij}(\mathbf{x}, \mathbf{k})$ are not necessarily real numbers. The Reynolds tensor symmetry in $(\mathbf{x}_1, \mathbf{x}_2)$-space,

$$R_{ij}(\mathbf{x}_1, \mathbf{x}_2) = R_{ji}(\mathbf{x}_2, \mathbf{x}_1),$$

translates into

$$R_{ij}(\mathbf{x}, \mathbf{k}) = R_{ji}(\mathbf{x}, -\mathbf{k}) = R_{ji}^*(\mathbf{x}, \mathbf{k}), \tag{A.2}$$

in which * denotes complex conjugate.

We consider how the Fourier transforms of terms in (2.2) can be expressed compactly. The operations of gradient and multiplication by coordinate transform as follows:

$$\frac{\partial}{\partial r_j} \to ik_j, \qquad r_j \to i\frac{\partial}{\partial k_j}. \tag{A.3}$$

Thus,

$$\frac{\partial}{\partial x_{1j}} = \frac{1}{2}\frac{\partial}{\partial x_j} + \frac{\partial}{\partial r_j} \to \frac{1}{2}\frac{\partial}{\partial x_j} + ik_j \tag{A.4a}$$

and

$$\frac{\partial}{\partial x_{2j}} = \frac{1}{2}\frac{\partial}{\partial x_j} - \frac{\partial}{\partial r_j} \to \frac{1}{2}\frac{\partial}{\partial x_j} - ik_j. \tag{A.4b}$$

For example, the transformed incompressibility conditions, 2.4, are

$$\left(\frac{1}{2}\frac{\partial}{\partial x_i}+ik_i\right)R_{ij}(\mathbf{x},\mathbf{k})=\left(\frac{1}{2}\frac{\partial}{\partial x_j}-ik_j\right)R_{ij}(\mathbf{x},\mathbf{k})=0. \tag{A.5}$$

To transform $u_n(\mathbf{x}_1)R_{ij}(\mathbf{x}_1,\mathbf{x}_2)$, we first utilize Taylor's theorem in operator form to write

$$u_n(\mathbf{x}_1)=u_n(\mathbf{x}+\tfrac{1}{2}\mathbf{r})=\exp\left(\tfrac{1}{2}r_l\frac{\partial}{\partial x_l}\right)u_n(\mathbf{x}).$$

Thus,

$$\int e^{-i\mathbf{k}\cdot\mathbf{r}}u_n(\mathbf{x}_1)R_{ij}(\mathbf{x}_1,\mathbf{x}_2)\,d\mathbf{r}=\Sigma(\mathbf{x},\mathbf{k})u_n(\mathbf{x})R_{ij}(\mathbf{x},\mathbf{k}), \tag{A.6}$$

where $\Sigma(\mathbf{x},\mathbf{k})$ denotes a differential operator in both $\mathbf{x}$- and $\mathbf{k}$-space:

$$\Sigma(\mathbf{x},\mathbf{k})=\exp\left(\frac{i}{2}\frac{\partial^{(u)}}{\partial x_l}\frac{\partial}{\partial k_l}\right).$$

The superscript (u) on the $\mathbf{x}$-gradient specifies that this gradient operates on $u_n(\mathbf{x})$, but not on $R_{ij}(\mathbf{x},\mathbf{k})$ in (A.6). One approach to evaluation of the right-hand side of (A.6) is to expand $\Sigma(\mathbf{x},\mathbf{k})$ in series

$$\Sigma(\mathbf{x},\mathbf{k})=\sum_{m=0}^{\infty}\left(\frac{i}{2}\frac{\partial^{(u)}}{\partial x_l}\frac{\partial}{\partial k_l}\right)^m\frac{1}{m!} \tag{A.7}$$

and apply the multiple derivatives to u_nR_{ij}.

We see that, under the Fourier transform,

$$-\nabla_1^2\to-\left(\frac{1}{2}\frac{\partial}{\partial x_l}+ik_l\right)^2=e^{-2i\mathbf{x}\cdot\mathbf{k}}(-\tfrac{1}{4}\nabla_x^2)e^{2i\mathbf{x}\cdot\mathbf{k}}.$$

Therefore, for Green's function of Section 2, (2.8), we have the transformed equation

$$-\left(\frac{1}{2}\frac{\partial}{\partial x_l}+ik_l\right)^2G(\mathbf{x}-\mathbf{x}',\mathbf{k})=\delta(\mathbf{x}-\mathbf{x}'),$$

and

$$G(\mathbf{x}-\mathbf{x}',\mathbf{k})=\frac{e^{-2i\mathbf{k}\cdot(\mathbf{x}-\mathbf{x}')}}{\pi|\mathbf{x}-\mathbf{x}'|}. \tag{A.8}$$

The transform of the Poisson equation for the pressure–velocity correlation, (2.2d), is to be derived with the transformed Green's function $G(\mathbf{x}-\mathbf{x}',\mathbf{k})$. We define, as an abbreviation,

$$\nabla_n(\mathbf{x},\mathbf{k})=\frac{1}{2}\frac{\partial}{\partial x_n}+ik_n, \tag{A.9}$$

so that $\nabla_n(\mathbf{x},\mathbf{k})$ and $\nabla_n^*(\mathbf{x},\mathbf{k})$ are the operator transforms of $\partial/\partial x_{1n}$ and $\partial/\partial x_{2n}$.

We have then, in $(\mathbf{x},\mathbf{k})$-space, an integral operator with kernel $G(\mathbf{x}-\mathbf{x}',\mathbf{k})$ and two differential operators $\Sigma(\mathbf{x},\mathbf{k})$ and $\nabla_n(\mathbf{x},\mathbf{k})$. $\Sigma(\mathbf{x},\mathbf{k})$ acts only on products of type $u_a(\mathbf{x})R_{bc}(\mathbf{x},\mathbf{k})$. The integral operator commutes with $\nabla_n(\mathbf{x},\mathbf{k})$ and with $\nabla_n^*(\mathbf{x},\mathbf{k})$ because ∇^2 commutes with $\partial/\partial x_{1j}$ and $\partial/\partial x_{2j}$ in $(\mathbf{x}_1,\mathbf{x}_2)$-space. The transform of (2.7) takes the form

$$\Pi_j(\mathbf{x},\mathbf{k})=\nabla_n(\mathbf{x},\mathbf{k})\nabla_m(\mathbf{x},\mathbf{k})\int G(\mathbf{x}-\mathbf{x}',\mathbf{k})\,d\mathbf{x}'[2\Sigma(\mathbf{x}',\mathbf{k})u_n(\mathbf{x}')R_{mj}(\mathbf{x}',\mathbf{k})+T_{mnj}(\mathbf{x}',\mathbf{k})]. \tag{A.10}$$

The mean flow equation, (2.6), is unchanged by the transformation to $(\mathbf{x},\mathbf{k})$-space except that, for the

Reynolds stress term, we can use

$$\langle u_i(\mathbf{x})u_n(\mathbf{x})\rangle_{,n} = \frac{\partial}{\partial x_n}\int \frac{R_{in}(\mathbf{x},\mathbf{k})\,d\mathbf{k}}{(2\pi)^3}. \tag{A.11}$$

Following the rules given above, we find that the transform of (2.2) can be written as

$$\frac{\partial}{\partial t}R_{ij}(\mathbf{x},\mathbf{k}) = A_{ij}(\mathbf{x},\mathbf{k}) - [B_{ij}(\mathbf{x},\mathbf{k}) + C_{ij}(\mathbf{x},\mathbf{k}) + 2D_{ij}(\mathbf{x},\mathbf{k}) + F_{ij}(\mathbf{x},\mathbf{k}) + H_{ij}(\mathbf{x},\mathbf{k})]^{\mathrm{S}}, \tag{A.12a}$$

where S indicates symmetrization by adding terms with $\mathbf{i}\leftrightarrow\mathbf{j}$, $\mathbf{k}\leftrightarrow -\mathbf{k}$, and

$$A_{ij}(\mathbf{x},\mathbf{k}) = -2\nu k^2 R_{ij}(\mathbf{x},\mathbf{k}) + \tfrac{1}{2}\nu\frac{\partial^2}{\partial x_l^2}R_{ij}(\mathbf{x},\mathbf{k}), \tag{A.12b}$$

$$B_{ij}(\mathbf{x},\mathbf{k}) = \nabla_n(\mathbf{x},\mathbf{k})\Sigma(\mathbf{x},\mathbf{k})u_n\mathbf{R}_{ij}(\mathbf{x},\mathbf{k}), \tag{A.12c}$$

$$C_{ij}(\mathbf{x},\mathbf{k}) = \nabla_n(\mathbf{x},\mathbf{k})\Sigma(\mathbf{x},\mathbf{k})u_i(\mathbf{x})R_{nj}(\mathbf{x},\mathbf{k}), \tag{A.12d}$$

$$D_{ij}(\mathbf{x},\mathbf{k}) = \nabla_i(\mathbf{x},\mathbf{k})\nabla_n(\mathbf{x},\mathbf{k})\nabla_m(\mathbf{x},\mathbf{k})\int G(\mathbf{x}-\mathbf{x}',\mathbf{k})\,d\mathbf{x}'\Sigma(\mathbf{x}',\mathbf{k})u_n(\mathbf{x}')R_{mj}(\mathbf{x}',\mathbf{k}), \tag{A.12e}$$

$$F_{ij}(\mathbf{x},\mathbf{k}) = \nabla_n(\mathbf{x},\mathbf{k})T_{inj}(\mathbf{x},\mathbf{k}), \tag{A.12f}$$

$$H_{ij}(\mathbf{x},\mathbf{k}) = \nabla_i(\mathbf{x},\mathbf{k})\nabla_n(\mathbf{x},\mathbf{k})\nabla_m(\mathbf{x},\mathbf{k})\int G(\mathbf{x}-\mathbf{x}',\mathbf{k})\,d\mathbf{x}'T_{mnj}(\mathbf{x}',\mathbf{k}). \tag{A.12g}$$

The equation is still exact. Each term on the right includes a different physical mechanism for changing R_{ij} in time, as described after (2.12). When $r_l(\partial/\partial x_l)$ acts on a function of $\mathbf{r}$ and $\mathbf{x}$, characterized by length scales L_T and L_M, it reduces the function's order of magnitude by L_T/L_M. The Fourier transform, acted on by $(\partial/\partial x_l)$ $(\partial/\partial k_l)$, is likewise reduced by (L_T/L_M). Thus, the effect of $\Sigma(\mathbf{x},\mathbf{k})$ defined in (A.7) on such functions might be simulated by only a few powers of $(\partial/\partial x_l)(\partial/\partial k_l)$ if $L_T/L_M < 1$. Of course, this is not a proof, but a guideline. If the important range of k-values in $R_{ij}(\mathbf{x},\mathbf{k})$ is $(L_T)^{-1} < k$, then the same interpretation might be applied to an operator such as

$$\frac{k_i}{k^2}\left(\frac{\partial}{\partial x_j}\right).$$

It follows that the terms of (A.12) containing $G(\mathbf{x}-\mathbf{x}',\mathbf{k})$ might be approximated by simpler ones containing a limited number of x-derivatives. Let (A.10) be recast as a formal operator expression:

$$\Pi_j(\mathbf{x},\mathbf{k}) = \left[-\left(ik_l + \frac{1}{2}\frac{\partial}{\partial x_l}\right)^2\right]^{-1}\nabla_n\nabla_m(2\Sigma u_n R_{mj} + T_{mnj}). \tag{A.13}$$

Set

$$\left[-\left(ik_l + \frac{1}{2}\frac{\partial}{\partial x_l}\right)^2\right]^{-1} \to \frac{1}{k^2}\left[1 - \frac{i}{k^2}k_l\frac{\partial}{\partial x_l} - \frac{1}{4k^2}\nabla_x^2\right]^{-1} \tag{A.14}$$

and expand in powers of $\mathbf{x}$-derivatives. Suppose now that both $\Sigma(\mathbf{x},\mathbf{k})$ and $G(\mathbf{x}-\mathbf{x}',\mathbf{k})$ are expanded in the indicated manner and only those terms of (A.12c–g) are retained that have no more than first-order $\mathbf{x}$-derivatives. The result, after a little algebra, is utilized in (2.12).

Appendix B. Reduction of the Turbulent Diffusion Terms

The contribution to $D\varepsilon/Dt$ arising from the turbulent diffusion of E is obtained by substituting the diffusion terms of the dK/dt and $d(K/L^m)/dt$ equations, respectively (5.10a) and (5.10c), into (5.12). Using $L = \alpha K^{3/2}/\varepsilon$ and $g_D = c_D I_D \alpha$, we have, for the turbulent diffusion (TD) part,

$$\left(\frac{D\varepsilon}{Dt}\right)_{\mathrm{TD}} = g_D\frac{\varepsilon}{K}\left[\frac{3m-2}{2m}\frac{\partial}{\partial x_n}\left(\frac{K^2}{\varepsilon}\frac{\partial K}{\partial x_n}\right) + \frac{1}{m}L^m\frac{\partial}{\partial x_n}\left(\frac{K^2}{\varepsilon}\frac{\partial}{\partial x_n}\frac{K}{L^m}\right)\right]. \tag{B.1}$$

Similarly, replacing D/Dt by $\partial/\partial x_n$ in (5.12),

$$\frac{\partial \varepsilon}{\partial x_n} = \frac{\varepsilon}{K}\left[\frac{3m-2}{2m}\frac{\partial K}{\partial x_n} + \frac{1}{m}L^m\frac{\partial}{\partial x_n}\left(\frac{K}{L^m}\right)\right]. \tag{B.2}$$

Solving (B.2) for $\partial(KL^{-m})/\partial x_n$ and inserting into (B.1),

$$\left(\frac{D\varepsilon}{Dt}\right)_{\text{TD}} = g_D\frac{\varepsilon}{K}\left[\frac{3m-2}{2m}\frac{\partial}{\partial x_n}\left(\frac{K^2}{\varepsilon}\frac{\partial K}{\partial x_n}\right) - \frac{3m-2}{2m}L^m\frac{\partial}{\partial x_n}\left(\frac{1}{L^m}\frac{K^2}{\varepsilon}\frac{\partial K}{\partial x}\right) + L^m\frac{\partial}{\partial x_n}\left(\frac{1}{L^m}\frac{K}{\varepsilon}\frac{K^2}{\varepsilon}\frac{\partial \varepsilon}{\partial x}\right)\right].$$

Let the terms in the brackets above be X_1, X_2, X_3. Then

$$X_1 + X_2 = -\frac{(3m-2)}{2m}\frac{K^2}{\varepsilon}\frac{\partial K}{\partial x_n}L^m\frac{\partial}{\partial x_n}\frac{1}{L^m} = \frac{3m-2}{2}\frac{K^3}{\varepsilon}\frac{\partial \log K}{\partial x_n}\frac{\partial \log L}{\partial x_n}$$

and

$$\begin{aligned} X_3 &= \frac{K}{\varepsilon}\frac{\partial}{\partial x_n}\left(\frac{K^2}{\varepsilon}\frac{\partial \varepsilon}{\partial x}\right) + \frac{K^2}{\varepsilon}\frac{\partial \varepsilon}{\partial x_n}\frac{\partial}{\partial x_n}\left(\frac{K}{\varepsilon}\right) + \frac{K^3}{\varepsilon^2}\frac{\partial \varepsilon}{\partial x}L^m\frac{\partial}{\partial x_n}\frac{1}{L^m} \\ &= \frac{K}{\varepsilon}\frac{\partial}{\partial x}\left(\frac{K^2}{\varepsilon}\frac{\partial \varepsilon}{\partial x}\right) + \frac{K^3}{\varepsilon}\frac{\partial \log \varepsilon}{\partial x_n}\frac{\partial \log(K/\varepsilon)}{\partial x_n} - m\frac{K^3}{\varepsilon}\frac{\partial \log \varepsilon}{\partial x_n}\frac{\partial \log L}{\partial x_n}. \end{aligned}$$

Using $K^{3/2} = \varepsilon L/\alpha$ to eliminate $\log K$ in favor of $\log \varepsilon$ and $\log L$ in $X_1 + X_2$ and X_3, we get

$$\begin{aligned} \left(\frac{D\varepsilon}{Dt}\right)_{\text{TD}} &= g_D\left(\frac{\varepsilon}{K}\right)(X_1 + X_2 + X_3) \\ &= g_D\frac{\partial}{\partial x_n}\left(\frac{K^2}{\varepsilon}\frac{\partial \varepsilon}{\partial x_n}\right) - \frac{g_D K^2}{3}\left[\left(\frac{\partial \log \varepsilon}{\partial x_n}\right)^2 + (2-3m)\left(\frac{\partial \log L}{\partial x_n}\right)^2\right] \end{aligned} \tag{B.3}$$

from which the g_D terms of (5.13b) follow directly.

References

Basdevant, C., Legras, B., Sadourny, R., and Beland, B. (1981). A study of barotropic model flows: intermittency, waves, and predictability. *J. Atmospheric Sci.*, **38**, 2305–2326.

Batchelor, G.R. (1953). *The Theory of Homogeneous Turbulence*, pp. 133–168. Cambridge University Press, Cambridge.

Bell, T.L., and Nelkin, M. (1977). Nonlinear cascade models for fully developed turbulence. *Phys. Fluids*, **20**, 345–350.

Bell, T.L., and Nelkin, M. (1978). Time-dependent scaling relations and a cascade model of turbulence. *J. Fluid. Mech.*, **88**, 369–391.

Bertoglio, J.P., and Jeandel, D.A. (1987). Simplified spectral closure for inhomogeneous turbulence: application to the boundary layer. In *Turbulent Shear Flows*, vol. 5, pp. 19–30. Springer-Verlag, New York.

Besnard, D.C., and Harlow, F.H. (1988). Turbulence in two-field incompressible flows. *Internat. J. Multiphase Flow*, **14**, 679–699.

Besnard, D.C., Harlow, F.H., Rauenzahn, R.M., and Zemach, C. (1990). Spectral Transport Model for Turbulence. Report LA-11821-MS, Los Alamos National Laboratory.

Bluman, G.W., and Cole, J.D. (1974). *Similarity Methods for Differential Equations.* Applied Mathematical Sciences, vol. 13. Springer-Verlag, New York.

Brachet, M.E., Meneguzzi, M., Politano, H., and Sulem, P.L. (1988). The dynamics of freely decaying two-dimensional turbulence. *J. Fluid. Mech.*, **194**, 333–349.

Bradshaw, P., Cebeci, T., and Whitelaw, J. (1981). *Engineering Calculation Methods for Turbulent Flow*, pp. 45–48. Academic Press, New York.

Brissaud, A., Frisch, U., Leorat, J., Lesieur, M., Mazure, A., Pouquet, A., Sadourny, R., and Sulem, P.L. (1973). Catastrophe Énergetique et nature de la turbulence. *Ann. Geophys.*, **29**, 539–546.

Clark, T. (1991). Spectral Self-Similarity in Homogeneous Anisotropic Turbulence. Report LA-12284-T, Los Alamos National Laboratory.

Clark, T., and Zemach, C. (1991). Evolution of turbulence spectra subjected to homogeneous shear in transient and self-similar regimes. *Bull. Amer. Phys. Soc.*, **36**, 2686.

Comet-Bellot, G., and Corrsin, S. (1966). The use of a contraction to improve the isotropy of grid-generated turbulence. *J. Fluid Mech.*, **24**, 656–682.

Daly, B., and Harlow, F.H. (1970). Transport equations in turbulence. *Phys. Fluids*, **13**, 2634–2649.

Dannevik, W.P., Yakhot, V., and Orszag, S.A. (1987). Analytical theories of turbulence and the ε expansion. *Phys. Fluids*, **30**, 2021–2029.

De Kármán, T., and Howarth, L. (1938). On the statistical theory of isotropic turbulence. *Proc. Roy. Soc. London Ser. A*, **164**, 192–215.

Desniansky, V.N., and Novikov, E.A. (1974a). Simulation of cascade processes in turbulent flows. *Prikl. Mat. Mekh.*, **38**, 507–513 (English transl. *J. Appl. Math. Mech.*, **38**, 468–475).

Desniansky, V.N., and Novikov, E.A. (1974b). Evolution of turbulence spectra toward similarity. *Izv. Akad. Nauk SSSR Ser. Fiz. Atmospher. Okeana*, **10**, 127–136 (English transl. *Izv. Acad. Sci. USSR Atmospher. Ocean. Phys.*, **10**, 127–136).

Gilbert, A.D. (1988). Spiral structures and spectra in two-dimensional turbulence. *J. Fluid Mech.*, **193**, 475–497.

Gilding, B.H. (1980). On a class of similarity solutions of the porous media equation, III. *J. Math. Anal. Appl.*, **77**, 381–402.

Gilding, B.H., and Peletier, L.A. (1977). On a class of similarity solutions of the porous media equations, II. *J. Math. Anal. Appl.*, **57**, 522–538.

Gore, R.A., Harlow, F.H., and Zemach, C. (1991). Computation of mixing layers by a spectral transport model. *Proc. Eighth Symposium on Turbulent Shear Flows*, Munich, Section 29–2, pp. 1–6.

Heisenberg, W. (1948). Zur statistichen theorie der turbulenz. *Z. Phys.*, **124**, 628–657.

Herring, J.R., and Mcwilliams, J.C. (1985). Comparison of direct numerical simulation of two-dimensional turbulence with two-point closure: the effects of intermittency. *J. Fluid Mech.*, **153**, 229–242.

Kolmogorov, A.N. (1941). The local structure of turbulence in incompressible viscous fluid for very large Reynolds numbers. *Dokl. Akad. Nauk SSSR*, **30**, 301–305 (in English).

Kovasznay, L.G.S. (1948). Spectrum of locally isotropic turbulence. *J. Aero. Sci.*, **15**, 745–753.

Kraichnan, R.H. (1967). Inertial ranges in two-dimensional turbulence. *Phys. Fluids*, **10**, 1417–1423.

Kraichnan, R.H. (1971). Inertial range transfer in two- and three-dimensional turbulence. *J. Fluid Mech.*, **47**, 525–535.

Kraichnan, R.H. (1987). An interpretation of the Yakhot–Orszak turbulence theory. *Phys. Fluids*, **30**, 2400–2405.

Launder, B.E., and Spalding, D.B. (1972). *Mathematical Models of Turbulence*. Academic Press, New York.

Lander, B.E., and Spalding, D.B. (1974). The numerical computation of turbulent flows. *Comput. Methods Appl. Mech. Engrg.*, **3**, 269–289.

Launder, B.E., Morse, A., Rodí, W., and Spalding, D.B. (1972). The prediction of free shear flows—a comparison of performance of six turbulence models. *Proceedings of NASA Conference on Free Shear Flows*, vol. 1, pp. 361–526. Langley Press.

Launder, B.E., Reece, G.J., and Rodi, W. (1975). Progress in the development of a Reynolds stress turbulent closure. *J. Fluid Mech.*, **68**, 537–566.

Leith, C.E. (1967). Diffusion approximation to inertial energy transfer in isotropic turbulence. *Phys. Fluids*, **10**(7), 1409–1416.

Leith, C.E. (1968). Diffusion approximation for two-dimensional turbulence. *Phys. FLuids*, **11**, 671–673.

Lesieur, M. (1987). *Stochastic and Numerical Modeling*. Nijhoff, Boston.

Lesieur, M., and Schertzer, D. (1978). Amortissement autosimilaire d'une turbulence a grand nombre de Reynolds. *J. Méc.*, **17**, 609–636.

Menoret, L. (1982). Contribution à 1' étude spectral des écoulements turbulents faiblements inhomogènes et anisotropes. Thèse, Univ. Cl. Bernard, Lyon I.

Mohamed, M.S., and LaRue, J.C. (1990). The decay power in grid-generated turbulence. *J. Fluid Mech.*, **219**, 195–214.

Rose, H.A., and Sulem, P.L. (1978). Fully developed turbulence and statistical mechanics, *J. Physique*, **39**, 441–484.

Schiestel, R. (1987). Multiple-time-scale modeling of turbulent flows in one-point closures. *Phys. Fluids*, **30**, 722–731.

Warhaft, Z. (1980). An experimental study of the effect of uniform strain on thermal fluctuations on grid-generated turbulence. *J. Fluid Mech.*, **99**, 545–573.

Warhaft, Z., and Lumley, J.L. (1978). An experimental study of decay temperature fluctuations in grid generated turbulence. *J. Fluid Mech.*, **88**, 659–684.

Yakhot, V., and Orszag, S.A. (1986). Renormalization group analysis of turbulence, I. basic theory. *J. Sci. Comput.*, **1**, 3–51.

Yoshizawa, A. (1984). Statistical analysis of the deviation of the Reynolds stress from its eddy-viscosity representation. *Phys. Fluids*, **27**(6), 1377–1387.

Yoshizawa, A. (1987). Statistical modeling of a transport equation for the kinetic energy dissipation rate. *Phys. Fluids*, **30**, 628–631.